CHAPTER IV
RESULTS AND DISCUSSION

4.1 Surface modification of carbon nanotubes

In this set of experiments, the modification of multiwall carbon nanotubes (MWCNTs) by noncovalent surface modification was performed because this approach provided good dispersion and stability in aqueous solution while maintaining the integrity of CNT. However, the modified MWCNTs with various degree of deacetylation of chitosan by noncovalent surface modification were not adequate to provide their stability in aqueous solution. Therefore, covalent surface modification was needed to modify MWCNTs in smaller diameter to provide charged surface and short lengths of MWCNTs. To increase charged density and obtain different functional groups on MWCNTs surface, polyelectrolyte; PDADMAC and PSS, were selected to deposit on treated MWCNT by layer-by-layer self assembly technique with simplified method. The satisfied dispersion and stability properties of modified MWCNT were an important reason that MWCNT can be possibly integrated as a drug carrier for drug delivery application.

4.1.1 Noncovalent surface modification of multiwall carbon nanotubes with various degree of deacetylation of chitosan

Chitosan biopolymer was selected as a dispersing agent to modify nanotubes surface because of their biocompatibility and nontoxic. Generally, chitosan has been proposed to improve CNT dispersion before being applied in biosensor devices. Recently, chitosan and alginate were coated on singlewall carbon nanotubes surface by noncovalent surface modification and successfully load anticancer drug; doxorubicin onto them [73]. However, most of the publications the chitosan used, had a high degree of deacetylation (>80%) because it can easily be dissolved in aqueous solution. Degree of deacetylation (%*DD*) of chitosan was an important parameter that controlled the ratio of hydrophobic (N-acetyl-D-glucosamine) and hydrophilic (D-glucosamine) parts of chitosan structure [74, 75] (Figure 4.1). Degree of deacetylation of chitosan was calculated from the ratio of

D-glucosamine to total composition consist of N-acetyl-D- glucosamine and D-glucosamine.

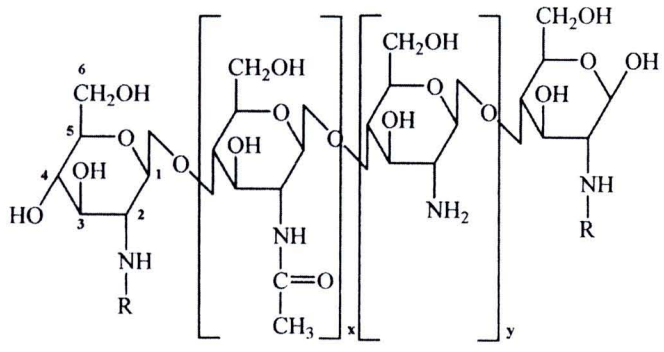

Figure 4.1 Chemical structure of Chitosan: x = N-acetyl-D-glucosamine unit, y = D-glucosamine unit: $x > 50\%$ = Chitin, $y > 50\%$ = Chitosan.

4.1.1.1 Chitosan synthesis

To control the hydrophobic/hydrophilic parts of chitosan by varying degree of deacetylation, the hydrophobic parts of chitosan were interesting key point to improve the chitosan adsorption efficiency on nanotubes surface while their stability in aqueous solution is still provided by hydrophilic parts. In the relevant literatures, the improvement of MWCNT's dispersion has been proposed with surfactant or polymer and even dye molecules by attaching hydrophobic part on nanotubes surface while the hydrophilic part stabilize modified MWCNT in aqueous solution. The hypothesis of our research was that the hydrophobic part of chitosan possibly attach on the nanotubes surface while the hydrophilic parts of chitosan stabilize carbon nanotubes in the aqueous solution.

Since chitosan with low *%DD* were not available as a commercial product, various degree of deacetylation of chitosan were needed to synthesize. Chitin, extracted from shrimp was deacetylated with concentrated sodium hydroxide at ambient temperature. When the reaction time was increased from 2 to 7 days, the degree of deacetylation of chitosan was increased as shown in Figure 4.2.

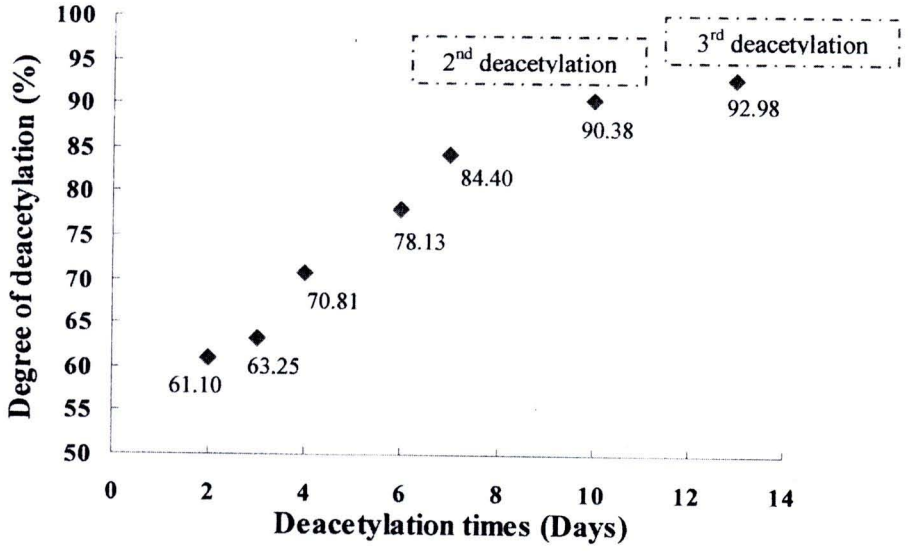

Figure 4.2 Plot of degree of deacetylation of chitosan which investigated by first derivative UV-Visible spectroscopy technique as a function of deacetylation time.

Under concentrated alkaline, sodium hydroxide reacted with chitin consist of N-acetyl-D-glucosamine as a repeating unit by nucleophilic substitution pathway, the acetyl groups become ammine groups and received sodium acetate as a by product as shown in Figure 4.3.

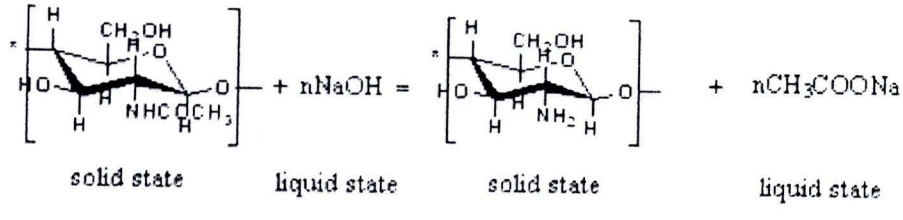

Figure 4.3 Schematic of deacetylated reaction of chitin under concentrated alkaline [76]

To receive the chitosan, the various reaction time from 2 to 7 days at ambient temperature can produce different %*DD* of chitosan in a range of 61% to

84 %*DD*. In addition, to increase degree of deacetylation of chitosan, the obtained chitosan from a reaction time of 7 days were reacted with fresh concentrated sodium hydroxide in the second and third rounds in order to deacetylate the remaining acetyl groups in their structure and receive the increasing of degree of deacetylation chitosan (90 and 93%*DD*). The obtained chitosan with different reaction time were investigated on degree of deacetylation of chitosan by first derivative UV-Vis spectroscopy technique.

Infrared spectroscopic method is commonly used to investigate the degree of deacetylation because it is relatively fast technique and does not require the dissolution of chitosan in aqueous solvent. The use of different baseline would inevitably contribute a variation in the degree of deacetylation value. Moreover, sample preparation, type of instrument and condition especially moisture might influence the sample analysis. Therefore, first derivative UV-Vis spectroscopy was selected instead of IR spectroscopy technique in order to solve this problem. The advantage of first derivative UV-Vis spectroscopy to investigate degree of deacetylation of chitosan was that it required only a small amount of sample and relied on simple reagent molecules. In addition, the method allowed a simple, convenient, time saving and was sensitive enough to detect the concentration of N-acetyl-D-glucosamine as low as 0.5 mg/l in 0.01 M acetic acid [77]. The results were reasonable with less interference of protein contaminants, which provided the good precision and accuracy for N-acetyl-D-glucosamine residue in chitosan.

Molecular weight of chitosan was another important parameter that should be considered because it might influence on adsorption efficiency as well. In this case, molecular weight of obtained chitosan was monitored using gel permeation chromatography (GPC). The results in Figure 4.4 showed that molecular weight was decreased in a range of 630 to 530 kDa when the reaction time increased at ambient temperature. Although the relevant literature has been reported that the synthesis temperature affect molecular weight especially at temperature over 40°C [78], in this case, in spite of different reaction time, the % difference of molecular weight of chitosan between 2 days and 13 days was slightly changed in 15.87 % when synthesized under ambient temperature. The nearly molecular weight of chitosan was the good point that we possibly neglected the effect of molecular weight of chitosan on MWCNTs dispersion.

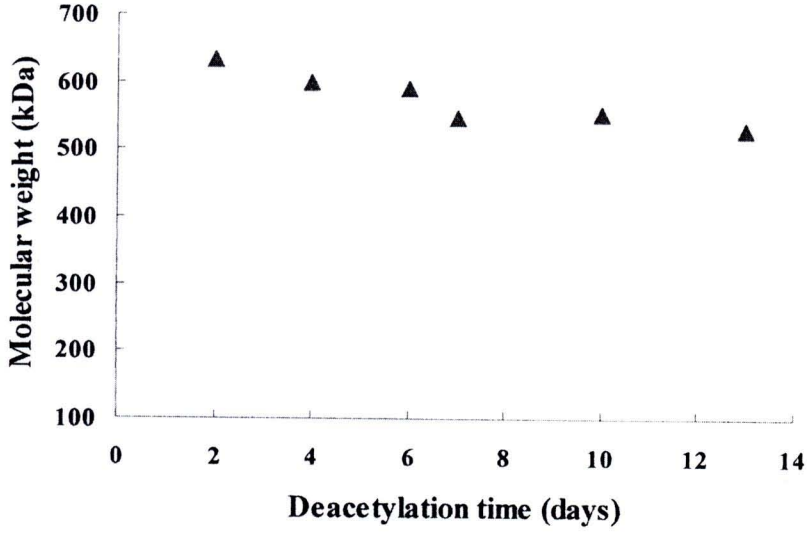

Figure 4.4 Molecular weight of chitosan as a function of deacetylation time

Therefore, the obtained chitosan with various degree of deacetylation (61, 71, 78, 84, 90 and 93 %DD) and molecular weight in a range of 630-530 kDa were used to noncovalently modify MWCNTs for improving their dispersion and stability in aqueous solution. The hypothesis of this experiment was that the hydrophobic parts (N-acetyl-D-glucosamine) of chitosan possibly attach on MWCNTs to separate to individual MWCNT while the hydrophilic parts (D-glucosamine) of chitosan stabilize MWCNTs by repel each other in aqueous solution as shown in Figure 4.5.

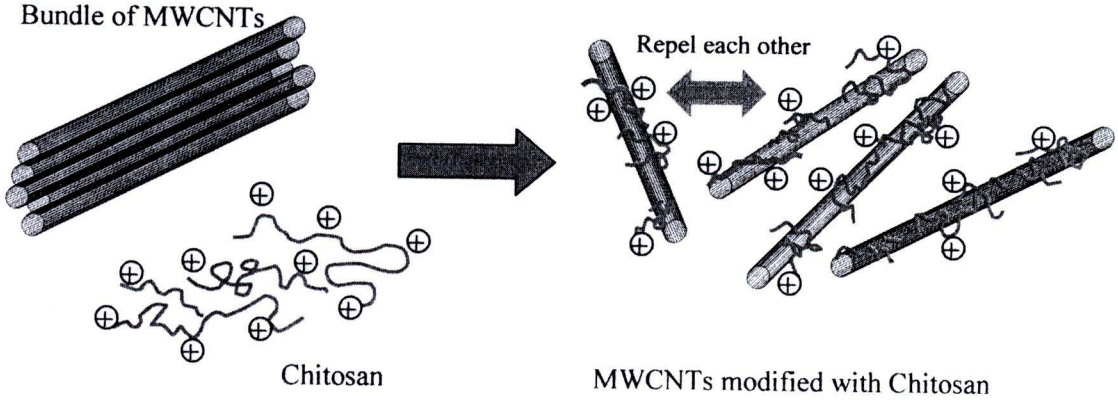

Figure 4.5 Hypothesis model of surface modification of MWCNTs with chitosan.

To achieve MWCNTs dispersion with chitosan, the sonication process was necessary step to temporarily disperse pristine MWCNTs in aqueous solution. Although pristine MWCNTs was sonicated, it was still hardly dispersed in solution because of their superhydrophobic property. Therefore, the diluted chitosan concentrration was used as a starting solution for increasing probability of pristine MWCNTs to attach the solution in order to disperse by sonicator.

4.1.1.2 Effect of sonication times on carbon nanotubes dispersion with chitosan

The sonication time is also affected to the pristine MWCNTs dispersion efficiency. The temporary dispersion of MWCNTs led the chitosan having time to attach on MWCNT surface. The increasing in sonication time increased the dispersion of MWCNTs by increasing the absorbance at 550 nm as shown in Figure 4.6. Until the sonication time reach to 30 minutes, the dispersion of MWCNTs was not significantly changed in absorbance. In addition, the lower %*DD* of chitosan provided the better dispersion than higher %*DD* because of the amount of hydrophobic parts. The carbon nanotubes are totally dispersed at sonication time 45 minutes. However, in the next experiment, we still used the minimum sonication time for 30 minutes in order to avoid the effect of increasing of temperature that heating up during the sonication process. Furthermore, low %*DD* as 61% chitosan provide high dispersion efficiency compare with chitosan 78 and 93%*DD*.

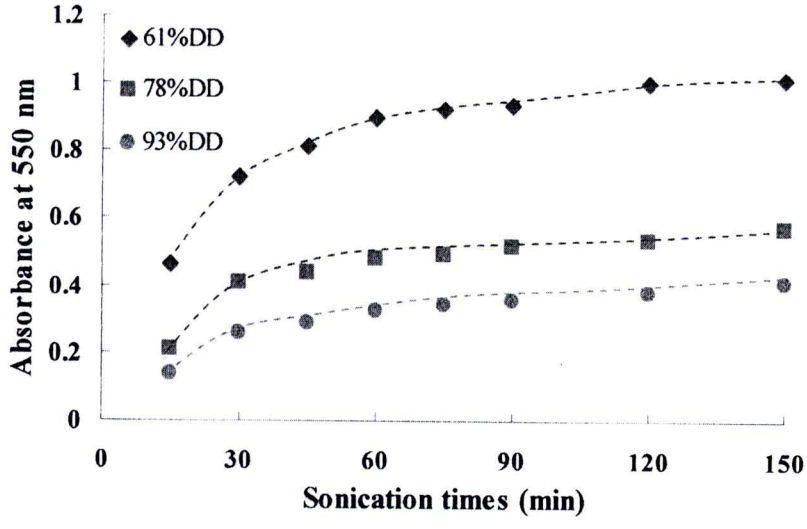

Figure 4.6 The dispersion of MWCNTs with 5 mM of different degree of deacetylation chitosan (61, 78 and 93%*DD*) as a function of sonication time.

4.1.1.3 Effect of chitosan concentration on carbon nanotubes dispersion

In these experiments, chitosan was used to disperse the MWCNTs by noncovalent surface modification. If one tries to disperse carbon nanotube in aqueous solution, it is well known that prior to the adjunction of any dispersing agent, the solution will appear clear with the MWCNTs aggregated at the air/water interface. Van der Waals attraction and π–π stacking between the abundant double bonds found in MWCNTs are through to be responsible for their aggregation and poor solubility in aqueous solution.

Shown in Figure 4.7 is a plot of the changes in absorbance of the solution as a function of the added chitosan concentration. From the initial solution of aggregated carbon nanotubes, as chitosan concentration is increased up to 1 mM, the adsorption of the polymer onto the carbon nanotubes leads to dispersion, which in turn leads to a sharp increase the absorbance at 550 nm. This increase in absorbance quickly levels off suggesting that all the carbon nanotubes, present in the solution, have been dispersed. Further increase of the chitosan solution to 9 mM does not induce any increase in

absorbance. When chitosan is added to the solution, noncovalent adsorption of chitosan on the nanotube surface is thought to take place, which initiate the dispersion by repulsion of the nanotubes. Since it has been reported that the acetyl groups represent the most hydrophobic part of the chitosan, the authors suggest that these functional groups could adsorb preferentially on the surface of the MWCNTs. In the mean time, the hydrophilic parts of chitosan (NH_3^+) induce a positive charge at the vicinity of the nanotubes surface, which allow their stabilization in aqueous solution by electrostatic repulsion. This dispersion process can be studied using UV–Visible spectroscopy by recording the changes in absorbance of the solution at 550 nm, and is therefore equivalent to a turbidity measurement. As carbon nanotubes absorb all the wavelengths in the visible part of the electromagnetic spectrum, increases in dispersion of the carbon nanotubes render the solution more and more pitch-black.

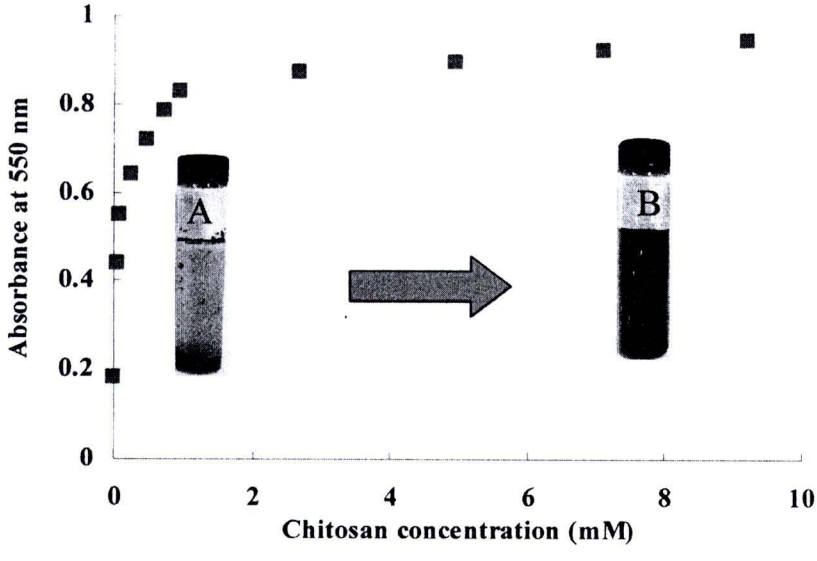

Figure 4.7 Plot of the changes in absorbance of a MWCNT solution as function of the 61%*DD* chitosan concentration (0-10mM).

4.1.1.4 Effect of degree of deacetylation of chitosan on carbon nanotubes dispersion

Since our hypothesis was that the more hydrophobic acetyl groups present in chitosan might allow a better interaction with the MWCNTs, our interest turned toward the preparation of chitosan having a higher molar fraction of acetyl groups thus a lower %*DD*.

Our hypothesis was that when the hydrophobic character of chitosan is controlled by the fraction of acetylated functional groups, chitosan with a lower %*DD* should be a better molecule for the dispersion of MWCNTs. Chitosan with a lower %*DD* can simply be prepared by a shorter reaction time of the chitin biopolymer in the 50% w/w sodium hydroxide solution.

In our work, we chose to use 61%*DD* chitosan as the lowest degree of deacetylation because the resulting chitosan molecules were not sufficiently soluble and led to very scattered results. Shown in Figure 4.8 (squares), is the absorbance of different solutions containing MWCNTs dispersed with chitosan having different degree of deacetylation (61, 71, 78, 84, 90 and 93%*DD*). Although it was shown in Figure 4.7 that a 1 mM chitosan concentration is sufficient to dispersed carbon nanotubes, a concentration of 5 mM chitosan was used to insure total dispersion of the MWCNTs in an excess solution of chitosan. From the absorbance measurements of the solutions, it can be seen that the efficiency of the dispersion of the carbon nanotubes, decrease when increasing the chitosan %*DD*. The final absorbance of the solution when using 61%*DD* is double than when using the 93%*DD* chitosan. These results suggest that, as expected, more hydrophobic chitosan segments found in the lower 61%*DD* are more efficient to adsorb onto the MWCNTs leading to a better dispersion of the carbon nanotube in solution. The mechanism through which CNT interact with chitosan is though to be due to hydrophobic interaction from hydrocarbon backbones and acetyl groups, and π system of the MWCNTs. CH–π interaction which is a weak hydrogen bonding attraction between soft acid C–H bond and soft base π system are also though to take part in the adsorption of chitosan onto the MWCNTs [79]. At low degree of deacetylation 61%*DD*, the bonding force between chitosan and MWCNTs is based on hydrophobic interaction

due to the acetyl groups that can interact with the surface of the nanotubes. For higher degree of deacetylation from 71%*DD* to 93%*DD*, the dispersion efficiency of the MWCNTs decreases due to the more hydrophilic character of the high %*DD* chitosan which is more soluble.

The efficiency of the surface modification of MWCNTs is often evaluated in term of stability against aggregation and sedimentation. Sedimentation occurs when the repulsion between MWCNTs is not strong enough to prevent the aggregation of the nanotube, leading to their precipitation. After surface modification of the MWCNTs by chitosan, the excess surface charges provided by the amino groups on the chitosan induce nanotube–nanotube repulsion and therefore prevent sedimentation. In our experiment, the sedimentation of the MWCNTs was accelerated with a centrifuge having a rotation rate of 2000 rpm for 10 minutes. In Figure 4.8 (triangles), is shown the absorbance of each MWCNTs solutions after centrifugation for each %*DD*. When compared to the initial absorbance (Figure 4.8, squares), a much lower absorbance as a result of the accelerated sedimentation by centrifugation was measured. Yet, it is interesting to observe that the lower 61%*DD* perform again better than the higher 93%*DD* although the former present a lower charge density when compare with the later. This would suggest that the adsorption of the lower %*DD* chitosan is greater than for higher %*DD*.

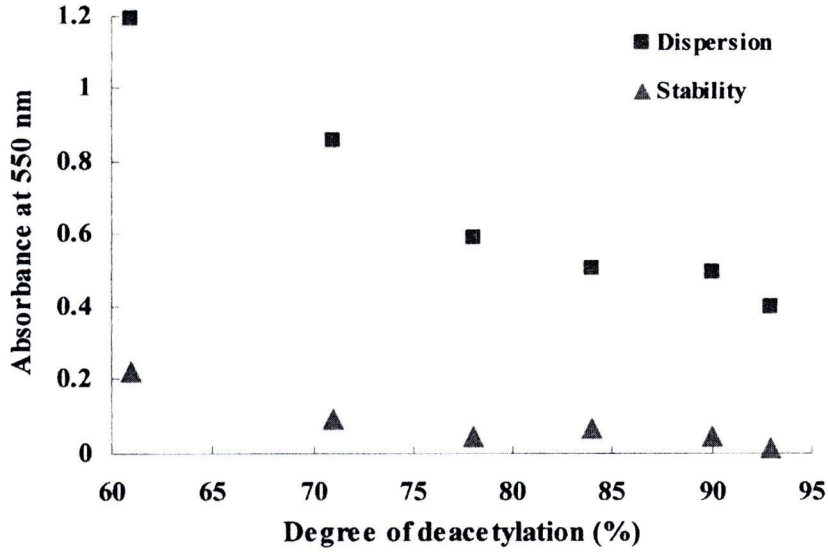

Figure 4.8 Plots of the changes in absorbance of a dispersion of MWCNTs in a 5 mM chitosan solution of various degree of deacetylation before (squares) and after (triangles) centrifugation at 2000 rpm for 10 minutes.

4.1.1.5 Surface charge of modified carbon nanotubes with different degree of deacetylation of chitosan

In term of resistance to sedimentation, this improved stability suggests that the MWCNTs modified with the lower %*DD* have a higher surface charge density, which provides a better stability against sedimentation. In order to access the value of the surface charge, we further characterized the MWCNTs surface by zeta potential measurements.

The surface charge density of colloidal particles dispersed in solution can be estimated by measuring the zeta potential, which represents the difference in potential between the slip plane of the double layer near the particles surface and the bulk solution. The zeta potential of the pristine carbon nanotube is expected to be initially nearly neutral but should become largely positive after adsorption of chitosan due to the presence of cationic amino groups. In our experiments, zeta potential values of the modified MWCNTs were ranging from 34 to 42 mV, which confirm the successful immobilization

of chitosan on the MWCNTs. Shown in Figure 4.9 (circles), the zeta potential values are plotted as a function of the %*DD*, which range from 42 mV (61%*DD*) to 34 mV (93%*DD*). These values decrease with increasing %*DD* and suggest that all MWCNTs dispersed in solutions have similar surface charged. Yet, because the 61%*DD* chitosan has a lower linear charge density when compared to 93%*DD*, these values need to be corrected if we want to compare the amount of polymer adsorbed at the surface of the MWCNTs. This lower linear charge density is due to the fact that the 61%*DD* contain only 61 groups for 100 monomers while the 93%*DD* contain 93 per 100 monomers.

Since the zeta potential is proportional to the density of charges, equal zeta potential for two nanotubes would require 1.5 times more 61%*DD* than 93%*DD* chitosan. Therefore the 93%*DD* has a linear charge density 1.5 times higher than the 61%*DD*. In Figure 4.9 (triangles) is plotted the corrected normalized chitosan monomer ration adsorbed onto the MWCNTs for each %*DD*. This plot is obtained by dividing the measured zeta potential by the corresponding %*DD* of the chitosan used and normalized. From the plot it can be seen that 1.9 times more 61%*DD* chitosan adsorb onto the MWCNTs when compared with the 93%*DD*. Several factors can justify the much lower adsorption of the 93%*DD* when compared with the 61%*DD*. The 93%*DD* has a better solubility, which means it will tend to remain in solution and will be more thermodynamically stable in solution. The higher charge density on the 93%*DD* chitosan can induce electrostatic repulsion of the groups, which in turn would lead to lower adsorption density of the chitosan while the 61%*DD* could adsorb in a more packed fashion.

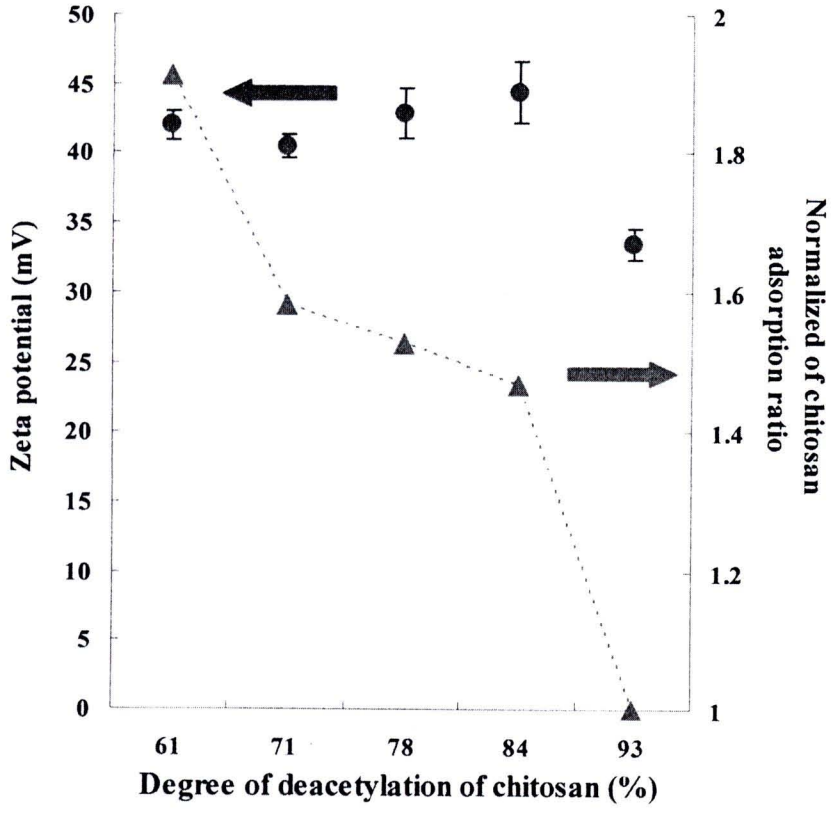

Figure 4.9 Zeta potential of modified MWCNT (circles) and normalized chitosan adsorption ratio onto the MWCNT (triangles) as a function of the %*DD* of chitosan.

Multiwall carbon nanotubes have been noncovalently modified with chitosan having different %*DD*. Using chitosan having different %*DD* had a strong effect on the quality of the nanotubes dispersion. UV–Visible spectroscopy results suggest that the nanotubes dispersion was improved when using chitosan with a lower degree of deacetylation (61%*DD*) when compared with higher degree of deacetylation (93%*DD*). The MWCNT modified with the lower %*DD* also displayed the best stability against centrifugation. Zeta potential measurements finally confirmed that the amount of chitosan adsorbed onto the nanotubes surface was twice as high with the lower %*DD* as with the high %*DD*. These modified MWCNTs with chitosan biopolymer could be used for the immobilization of hydrophobic and hydrophilic drug for drug delivery application.

4.1.2 Molecular Dynamics Simulation: Dispersion and seperation of chitosan wrapping on SWCNTs by noncovalently modification.

In our previous experiment, MWCNTs were modified with chitosan having different degree of deacetylation by noncovalent surface modification. The conclusion of this work was that low %*DD* as 61% of chitosan provided the best dispersion efficiency of MWCNTs. However, during modification process, pitch black mixture solution of MWCNT and chitosan still consist of two species which were the sedimentary CNT and stabilized CNT. As the behavior of modified MWCNTs with chitosan when it dispersed in the aqueous solution is not clearly known yet, molecular dynamics simulation was used to understand the behavior of dispersion and sedimentation of CNTs during modification process.

Molecular dynamics simulation was used to predict the interaction between singlewall carbon nanotubes (SWCNTs) and 60%*DD* of chitosan and interaction of modified CNTs with 60%*DD* of chitosan. Molecular dynamics simulation done on the three models: *i*) two pristine CNTs (*p*CNT-*p*CNT), *ii*) a pristine CNT–a chitosan-wrapped CNT (*p*CNT-*cw*CNT) and *iii*) two chitosan wrapped CNTs (*cw*CNT-*cw*CNT) as shown in Figure 4.10.

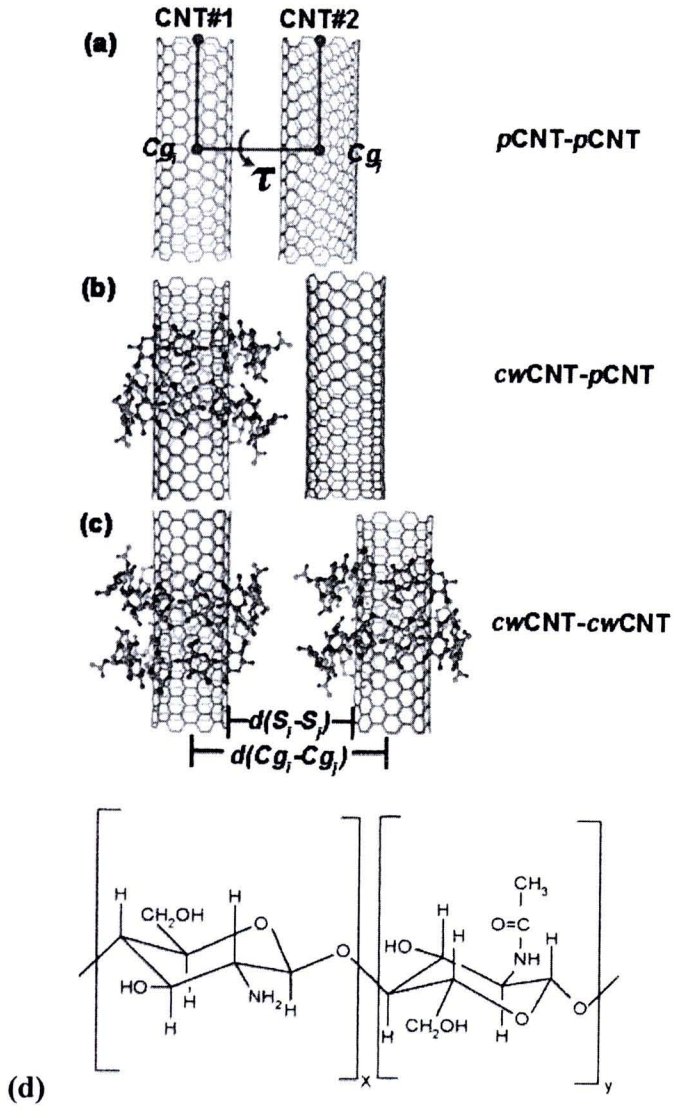

Figure 4.10 Schematic views of (a) two pristine CNTs (*p*CNT-*p*CNT), (b) a pristine CNT – a wrapped CNT with chitosan (*p*CNT-*cw*CNT), and (c) two chitosan-wrapped CNTs (*cw*CNT-*cw*CNT) where the SWCNT and the polymer used are the (8,8) armchair and 60%*DD* chitosan, respectively. The distances (*d(Cgi-Cgj)*) and (*d(Si-Sj)*) and torsion angle (τ) between the two SWCNTs were defined through the center of gravity (*Cg*) and the surface of each tube in which $\tau = 0°$ and the two tubes are parallel. The molecular structure of the chitosan's repeating units was shown (d).

4.1.2.1 Dispersion and solubility of CNTs

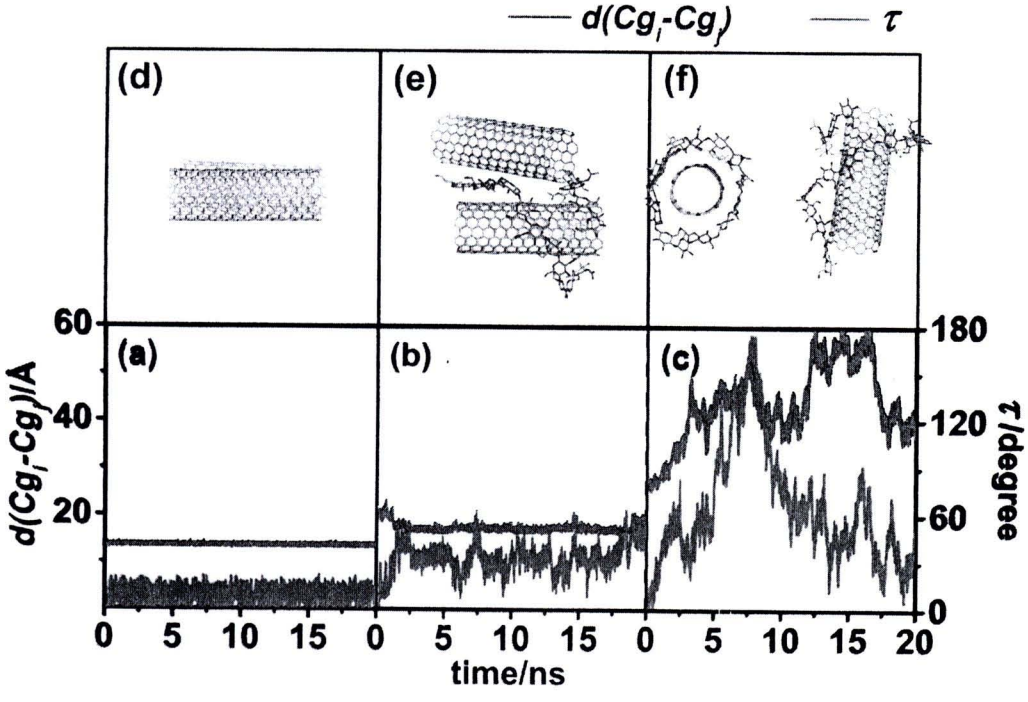

Figure 4.11 Distance (blue line), $d(Cg_i\text{-}Cg_j)$, between the two centers of gravity of SWCNT and torsion angle (red line), τ (see Figure 4.10 for definition), as a function of the simulation time for the three systems, (a) *p*CNT-*p*CNT, (b) *p*CNT-*cw*CNT and (c) *cw*CNT-*cw*CNT, where their corresponding structures taken from the MD simulation were also shown in (d), (e) and (f).

To understand the chitosan-assisted dispersion and separation of the CNTs in aqueous solution, the tube-tube displacement and orientation were monitored in terms of the distance from the center of gravity of tube i^{th} (Cg_i) to that of tube j^{th} (Cg_j), $d(Cg_i\text{-}Cg_j)$, and the torsion angle between the two SWCNTs' axis, τ, respectively (see Figure 4.10 for definitions). The calculated results were shown in Figure 4.11.

In the system of two pristine SWCNTs (*p*CNT-*p*CNT), the averaged tube-tube displacement represented by the between the centers of tube gravity, $d(Cg_i\text{-}Cg_j)$, is ~14 Å equivalent to that distance between the tube surfaces, $d(S_i\text{-}S_j)$, of 3 Å (Figure 4.11(a)). In addition, the tilt angle donated by τ angle is ~11°. All values are almost

constant over the period of simulation time. The τ data indicated that the two pristine SWCNTs were oriented in almost parallel configuration (Figure 4.11(d)) while the distance between the surfaces, $d(S_i\text{-}S_j)$, of the two tubes of ~3 Å implied that the hydrophobic and van der Waals interactions between the aromatic rings of both CNTs were observed to play role. This can be a clear answer why the pristine CNTs were found to aggregate experimentally in solution.

With low concentration of chitosan represented by the *p*CNT-*cw*CNT system, the $d(Cg_i\text{-}Cg_j)$ was increased by ~3 Å from 14 Å to 17 Å and the tilt angle was increased from 11° to 33°, relative to those of the *p*CNT-*p*CNT system. Interestingly, one end of the chitosan fragments was found to unwrap from one tube (CNT#1 in Figure 4.10(b)) and change its configuration to interact with another CNT (pristine, CNT#2 in Figure 4.10(b)), *i.e.*, the chitosan rearranges its conformation to locate in between both CNTs. Although the $d(Cg_i\text{-}Cg_j)$ distance of ~17 Å, with the corresponding $d(S_i\text{-}S_j)$ of ~6 Å, is rather long for molecular interactions but the detected CNT-chitosan-CNT configuration signifies that the chitosan fragments can act as the linker to hold the two tubes together. The simulated phenomenon was firmly supported by the experimental data where the CNT was found to participate in the low concentration of the 60%DD chitosan [80].

Situation is different for the system where both CNTs were wrapped by chitosan fragment, *cw*CNT-*cw*CNT. This supposes to represent the CNT in the solution of high concentration of chitosan. As the results, the two wrapped CNTs were found to separate totally and rotate freely, *i.e.*, the noncovalently modified CNTs is highly soluble. This fact was definitely supported by the $d(Cg_i\text{-}Cg_j)$ distance and the τ angle ranging from ~35-60 Å and ~60-180°, respectively (Figure 4.11 (c) and Figure 4.11 (f)). The dispersion and solubility of the two modified CNTs is mainly due to the strong repulsion between the positively charged ammonium groups on the glucosamine units of the chitosan.

4.1.2.2 Role of chitosan fragments

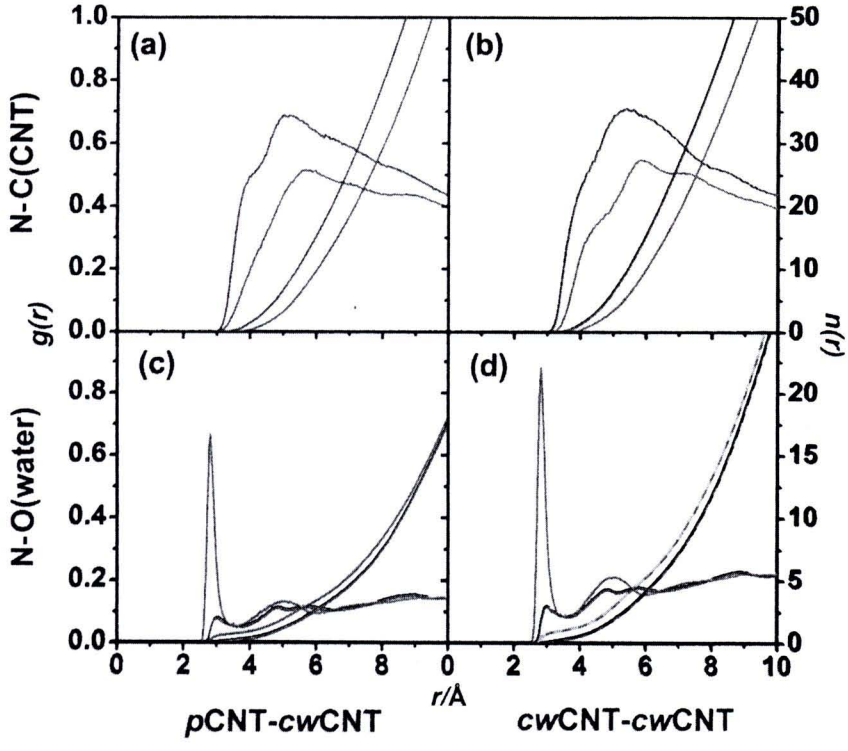

Figure 4.12 RDFs from the nitrogen atoms on the N-acetyl-D-glucosamine (N(NAG), blue line) and D-glucosamine (N(GLS), red line) of chitosan (see Figure 4.10(d) for definition) to the carbon atoms of the wrapped CNTs (a) CNT#1 for the *p*CNT-*cw*CNT, (b) both CNT#1 and CNT#2 for the *cw*CNT-*cw*CNT and (c) oxygen atoms of water.

According to our previous study on the chitosan-wrapped CNT, the aggregation of the surface modified CNT is possibly due to the hydrophobic interactions between the acetyl groups of chitosan and the aromatic rings of CNT. In order to provide detailed information at molecular level to understand the mechanism of action, the atom-atom radial distribution functions (*RDFs*, $g_{xy}(r)$), that is the probability of finding a particle of type y within a sphere radius r around the particle of type x, were calculated. Here, x represents the nitrogen atoms of chitosan fragments (the N-acetyl-D-glucosamine (NAG), and D-glucosamine (GLS)), and y denotes all the carbon atoms of the CNTs

(only the wrapped CNTs shown in Figure 4.10, CNT#1 for the *p*CNT-*cw*CNT and both CNT#1 and CNT#2 for the *cw*CNT-*cw*CNT systems) or the water oxygen atoms. The results were plotted and compared in Figure 4.12.

In the *p*CNT-*cw*CNT system (Figure 4.12(a)), the RDF plots from the N atom on the acetyl group of the NAG unit, N(NAG), and the ammonium group of the GLS unit, N(GLS), to all carbon atoms CNTs show broad maxima at 5.2 Å (blue line) and 5.7 Å (red line) with high and low intensities, respectively. This means that the acetyl group of NAG an approach closer to the outer surface of the tube than the ammonium group of GLS, *i.e.*, the hydrophobic acetyl group (NAG) better interacts with the two tubes through van der Waals interaction than the hydrophilic ammonium group (GLS), causing the CNT aggregation. As expected, the corresponding running integration number, number of water molecule at the distance *r*, around the neutral NAG (blue line) is higher than that of the positively charged GLS group (red line) at any distances. This is in consistent with the intensity of both plots that of the NAG at any distances is higher than that of the GLS groups.

Similarly for the *cw*CNT-*cw*CNT system (Figure 4.12(b)), the RDF for the NAG (5.6 Å, blue line) takes place at shorter distance than that of the GLS group (6.2 Å, red line) with higher density and higher coordination number. Interestingly, both N(NAG)-C(CNT) and N(GLS)-C(CNT) distances of 5.2 Å and 5.7 Å (Figure 4.12(a)) of the *p*CNT-*cw*CNT system are shorter than those of 5.6 Å and 6.2 Å (Figure 4.12(b)) of the *cw*CNT-*cw*CNT system, respectively. This fact can be described based on the molecular configurations shown in Figure 4.10(b) and 4.10(c), *i.e.*, the chitosan fragment in the high soluble chitosan-wrapped CNT (*cw*CNT-*cw*CNT) can be easily accessed by water molecules than that of the aggregated one (*p*CNT-*cw*CNT). Due to this solvation effect, the chitosan fragment in the *cw*CNT-*cw*CNT system was, then, pulled out to locate at longer distance than that of the *p*CNT-*cw*CNT one.

As expected, the positively charged N(GLS) atom was found to be much better solvated than the N(NAG) atom (Figure 4.12(c) and 4.12(d)). For both systems, *p*CNT-*cw*CNT and *cw*CNT-*cw*CNT, the RDFs for the N(GLS) are much sharper with much higher density than those of the N(NAG). The corresponding coordination numbers,

integrated to their first minima, of the N(GLS) for both systems of 0.9 is higher than that of 0.3 water molecules of the N(NAG) atom.

Molecular dynamics simulation approach was applied to investigate an increase in dispersion and solubility of single-walled carbon nanotube in solution by 60%*DD* chitosan noncovalently wrapped on the outer surface using the three models: *p*CNT-*p*CNT, *p*CNT-*cw*CNT and *cw*CNT-*cw*CNT. In the *p*CNT-*p*CNT and *p*CNT-*cw*CNT systems, the distance between the centers of tube gravity and the tube-tube orientation indicated the aggregation of carbon nanotube. This is due to the hydrophobic and van der Waals interactions between the aromatic rings of the two pristine CNTs, and the chitosan wrapped on CNT#1 acting as a linker interacted with both tubes, respectively. In contrast, the two *cw*CNTs were totally separated, freely rotated and well dispersed in aqueous solution owing to the charge-charge repulsive force of the ammonium groups of GLS, a fragment of 60%*DD* chitosan, wrapping on each tube. Interestingly, the hydrophobic acetyl group of NAG fragment is likely to interact with the aromatic rings of carbon nanotube via van der Waals interaction while the positively charged ammonium group of GLS fragment was strongly solvated by waters. These theoretical results can support the previous experimental work in the fact that the hydrophobic acetyl parts of chitosan favored to attach on the nanotubes surface while the hydrophilic ammonium parts provided nanotubes stabilize in the solution by charge-charge repulsive force to each others.

4.1.3 Covalent surface modification of multiwall carbon nanotubes with acid oxidation (H_2SO_4 and HNO_3)

The multiwall carbon nanotubes (MWCNTs) were oxidized by strong acid, H_2SO_4 and HNO_3, the oxidation reaction is known to generate various at the open end or the defect sites of carbon nanotubes structure, thereafter functional groups as follow -COOH, -OH, -C=O and another group as sulfur-containing might be introduced in the carbon nanotubes structure.

From the raman spectra of treated and pristine MWCNTs, the characteristic of carbon nanotubes, G band in 1600 cm^{-1}, and D band in 1300 cm^{-1} was shown in Figure

4.13. D band presents the amorpous carbon or disordered C in carbon nanotubes while G band was presents the C-C bond in graphene sheet. D́ band was presented the shoulder of G band that also induced the disordered C. The increasing in intensity of D band suggest disordered structure by carboxylation increased. The I_G/I_D ratio is used to the assess of the ratio of sp^2/sp^3. The ratio I_G/I_D of pristine MWCNTs equal to 0.5056 while the ratio I_G/I_D of treated MWCNTs equal to 0.2773. This suggests that D band was increased in case of treated MWCNTs because of carboxlic acid groups.

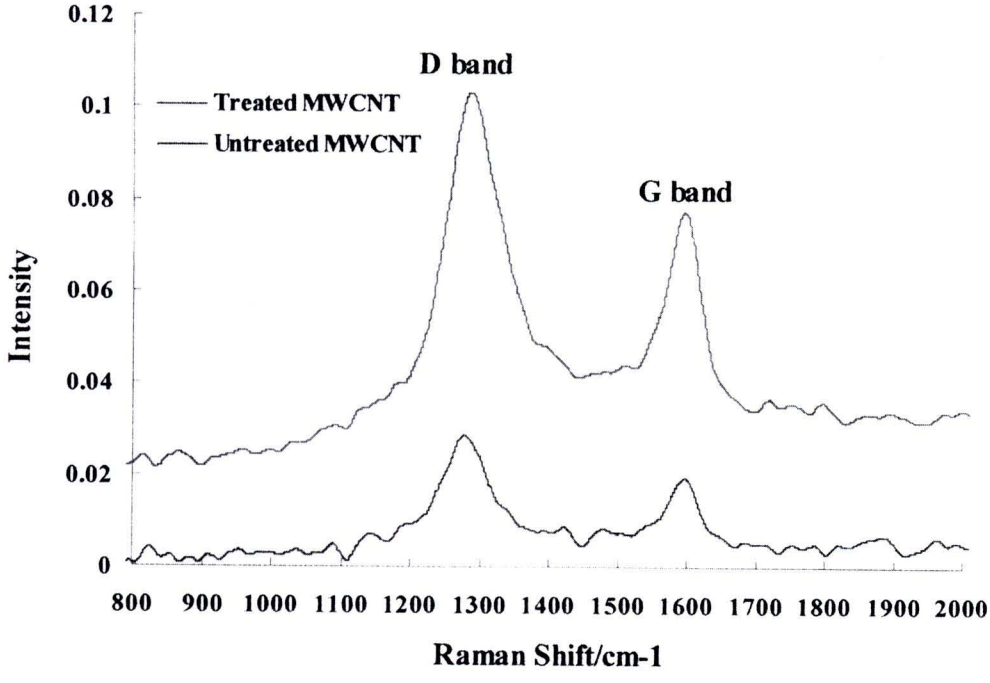

Figure 4.13 Raman spectra of pristine MWCNT and treated MWCNTs.

The results of FTIR transmission shown that the shoulder peak of carbonyl at 1710 cm^{-1} shown in Figure 4.14. Although the characteristic peak of carbon nanotubes was not shown clearly in different position, the intensity of the % transmission were increased in case of treated carbon nanotubes. In addition, the height peak of C-H stretching in 2845 and 2912 cm^{-1} decreased after treat MWCNTs with acid.

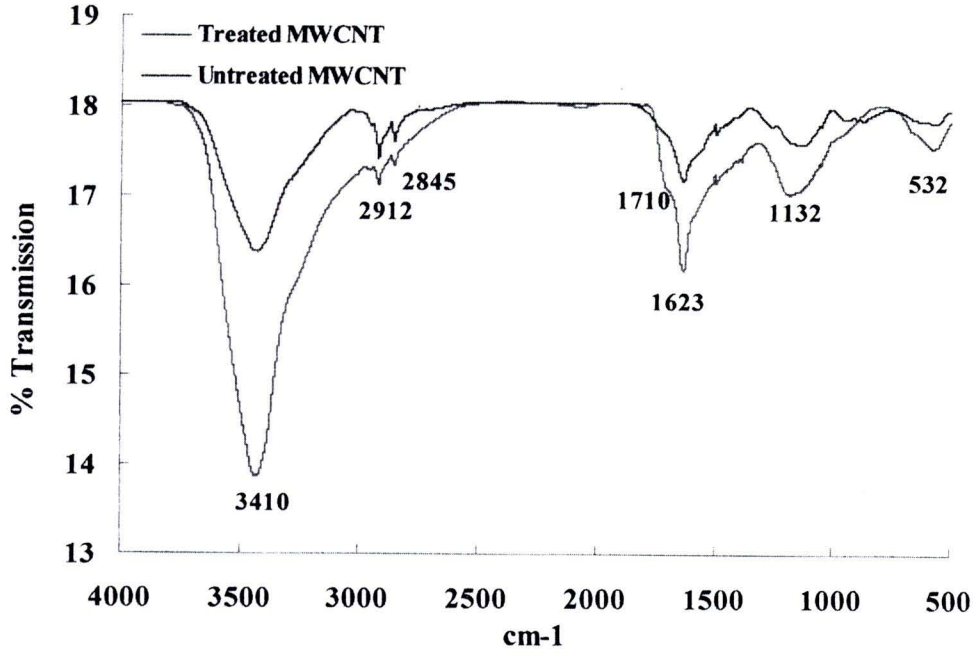

Figure 4.14 FTIR spectra of pristine MWCNT and treated MWCNTs.

To confirm the functional groups on treated MWCNT, especially carboxylic group, FTIR spectra show the evidence that, 3410 cm^{-1} is –OH stretching, 1710 cm^{-1} is C=O of carboxylic acid, 1623 cm^{-1} is C-C stretching of aromatic and 1132 cm^{-1} is C-O of carboxylic acid.

During the oxidation MWCNTs, treated MWCNTs not only have the functional groups on their surface but also obtained in the shorter length. This result was received from the sonication process and as shown in Fiugure 4.15.

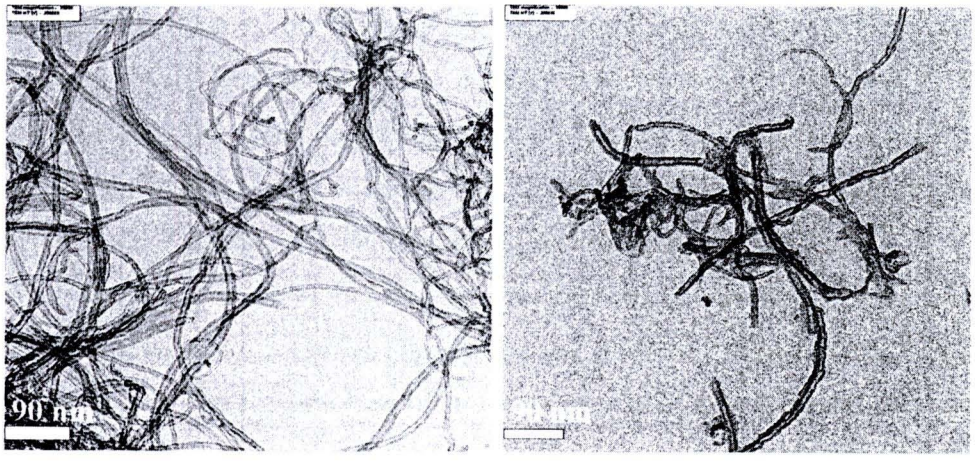

(a) (b)

Figure 4.15 Transmission electron micrograph of (a) pristine MWCNTs and (b) treated MWCNTs.

4.1.4 Layer-by-layer deposition on treated multiwall carbon nanotubes with polyelectrolyte; PDADMAC and PSS without centrifugation process

The key approach to provide good dispersion and improve the stability of CNT in aqueous solution is to develop a high anionic or cationic charge density at the surface of nanotube. Our previous work has been recently reported the improved adsorption of chitosan around CNT when the degree of deacetylation (%*DD*) of chitosan was lowered from 93%*DD* down to 61%*DD*. However, in term of the stability of modified MWCNTs with chitosan, it was insufficient to prepare as a drug carrier. Therefore, recent literature search is pointing toward a broader usage of the noncovalent surface modification of the nanotubes via layer-by-layer technique.

The functionalized CNT have been proposed by loading polyelectrolytes by layer-by-layer approach [81,82]. Layer-by-layer technique is a major breakthrough of noncovalent surface modification which has been used as a tool to construct polyelectrolyte multilayers with oppositely charged polyelectrolyte onto any type, shape and size of substrates even one dimension of nanomaterials as carbon nanotubes[29, 83].

To modify CNT surface via layer-by-layer technique, polyelectrolytes, enzyme, antibody, nucleic acid, proteins and nanoparticles such as gold and silver nanoparticles [84,85] have been successfully used to deposit on CNT. Moreover, after coating CNT with multilayers, modified CNT was utilized in a wide variety of applications such as a control release anticancer drug [40], cancer biomarker [39] and biosensor [38].

No matter what agent is used in the noncovalent surface modification, the methods usually rely on exposing the nanotubes solution to an excess of polymer followed by tedious centrifugation steps to remove the excess of unbound polymer from the solution. This method provide satisfying results with small volumes but the numerous centrifugation steps as well as the supernatant removal followed by re-dispersion make this method unpractical for scaling up to hundreds of milliliters of CNT solution.

Although this method provides satisfying results with small volumes, the major problem is that it can promote CNTs aggregation during centrifugation step because the carbon nanotubes are forced into dense pack [86]. In addition, the numerous centrifugation steps as well as the supernatant removal followed by re-dispersion make this method unpractical for scaling up to hundreds of milliliters of CNT solution. Moreover, significant amount of carbon nanotubes is lost during the removal of the supernatant. Filtration is another method which can be used to remove unbound polyelectrolyte through the membrane. This way is no forced modified carbon nanotubes into dense pack and it is not necessary to have a density difference between the particle and surrounding media [87]. However, the obstacle of this method is that it's hard to ensure that we can avoid the adsorption of excess polyelectrolyte even modified carbon nanotubes on the filter membrane during the solution pass through the filter membrane. Therefore, the amount of modified carbon nanotubes might possibly be lost during the filtration and re-dispersion process.

While working on the surface modification of MWCNT with biopolymer, our interest turned toward trying to find a simple method for the "just enough" surface modification of MWCNT by polyelectrolytes solution in order to remove the centrifugation step. Using this method, we have prepared up to 500 ml of MWCNT solutions in a single step but based on the proper adjunction of the polymer amount. Furthermore, the absence of polyelectrolyte excess in solution allowed for the utilizations

of the layer-by-layer deposition techniques with which up to tertiary layer of polyelectrolytes were successively deposited onto the MWCNT surface. The stability of modified MWCNT were identified by measuring turbidity of solution using UV-Visible spectroscopy at wavelength 550 nm combined with zeta potential measurements were used to evaluate and confirm the surface modification of the MWCNT.

4.1.4.1 Primary layer coating on treated MWCNTs with PDADMAC

4.1.4.1.1 Effect of PDADMAC concentration on the stability of treated MWCNTs

As they become more available, MWCNTs will be more present in commercial product and their preparation will need to be scaled up to large batches. The commonly used centrifugation of MWCNT post surface treatment will be unpractical and need to be replaced with simpler method. An alternative method to the previously described centrifugation procedure relies on the adjunction of the "just enough" polyelectrolyte to the MWCNT solution thus limiting the excess polyelectrolyte in solution to the minimum. In order to find the appropriate amount of PDADMAC that need to be added to each MWCNT solution, vials containing fixed amount of MWCNT were mixed with solution of increasing PDADMAC concentrations. The treated MWCNT were sonicated in order to temporarily overcome van der Waals attractive interactions and immediately mixed with the PDADMAC solutions. As the final concentration of PDADMAC was increased, the turbidity of the MWCNT dispersion was recorded by UV-Vis spectroscopy as evidence of the MWCNT stability.

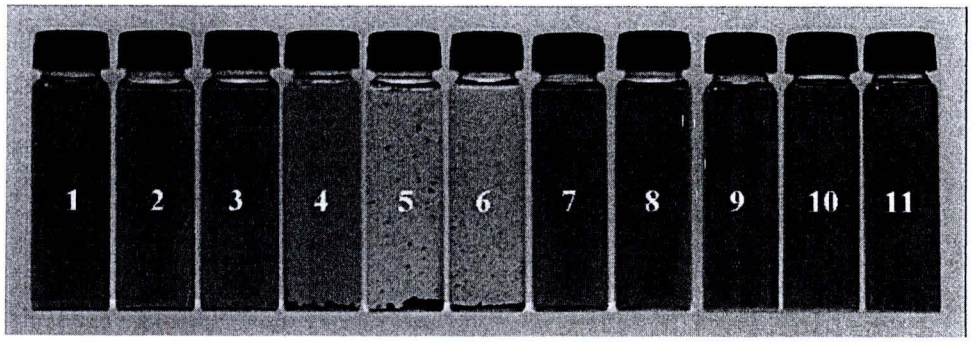
1
2
3
4
5
6
7
8
9
10
11

(a)

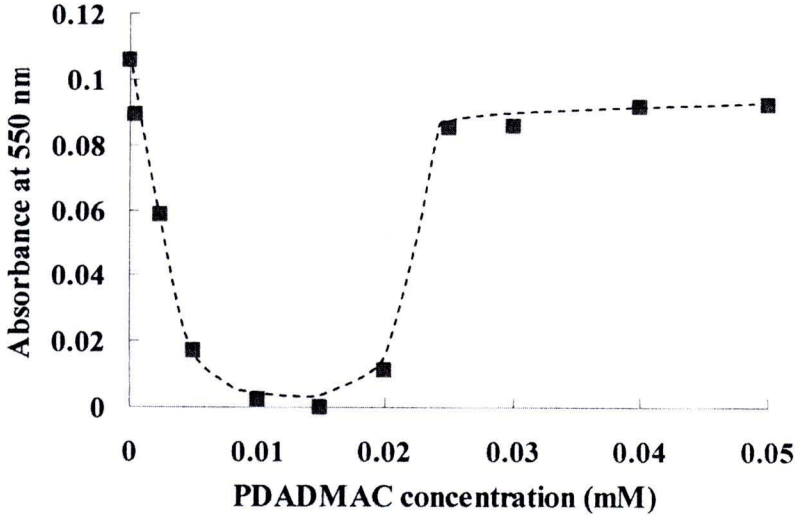
0.12
0.1
0.08
0.06
0.04
0.02
0
Absorbance at 550 nm
0
0.01
0.02
0.03
0.04
0.05
PDADMAC concentration (mM)

(b)

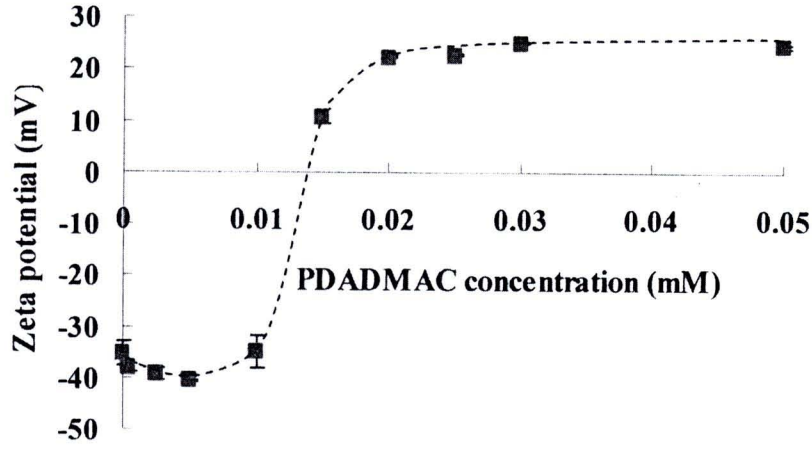

(c)

Figure 4.16 Stability of modified MWCNT 6.25 μg/ml with different poly(diallyldimethylammonium chloride) concentration (0-0.05 mM) (a) Solutions of treated MWCNT and the modified MWCNT with various PDADMAC concentrations, (b) Plots of the changes in absorbance of modified MWCNT with various PDADMAC concentration after preparing for 1 week, (c) Plots of reversal zeta potential of modified MWCNT with various PDADMAC concentrations.

Figure 4.16(a) showed pictures of the solutions corresponding to various added amount of PDADMAC (vial #2 to #11) compared with the original uncoated MWCNT in vial #1. It can be seen that when increasing the PDADMAC concentration from vial #2 to #6, the solution appeared clearer as the MWCNT precipitated. The appearance of a precipitate at low PDADMAC content is due to incompletely coverage of the surface of the anionic MWCNT. In this case, the two species present in solution are the anionic uncoated MWCNT and the cationic PDADMAC coated MWCNT that aggregate through electrostatic attraction and precipitate. Another reason that induce precipitation is because PDADMAC has large molecular weight (~200,000-350,000 g/mol) that can bind with different MWCNT (negatively charged MWCNT from treated MWCNT and in completely covered MWCNT) in solution and induce their bridged flocculation. Nevertheless, when the concentration of PDADMAC exceeds 0.025 mM as

shown vial #8, the MWCNT in solution remain dispersed with no precipitate appearing. All the MWCNT are then coated with the "primary" cationic PDADMAC layer.

UV-Vis spectroscopy was used to record the turbidity of the MWCNT/PDADMAC mixture at 550 nm as evidence of the CNT dispersion. The turbidity measurements are plotted in Figure 4.16(b) and a decrease in absorbance can be seen in the first section of the plot as the MWCNT precipitate out of the solution. Then, as the PDADMAC concentration was increased sufficiently to coat all the MWCNT, provide good dispersion and result in higher absorbance.

Figure 4.16(c) showed the corresponding zeta potential values for each of the prepared solutions. The zeta potential amplitude is proportional to the charge density at the nanoparticles surface and reflects successful adsorption of the charged polyelectrolytes and its sign corresponds to the anionic or cationic character of the surface. As expected, the zeta potential is reversed from negative for low PDADMAC concentration to positive values when PDADMAC is sufficiently adsorbed at the surface of the MWCNT. It can be seen that the initial negative charge due to the carboxylate is reversed to positive charge due to the presence quaternary ammonium of the PDADMAC. A lower absolute zeta potential value of +24 mV when compared to the -40 mV for the treated MWCNT is probably due to the low charge density of the PDADMAC as well as the fact that some negative carboxylic groups might remain from uncoated segment of the carbon nanotubes.

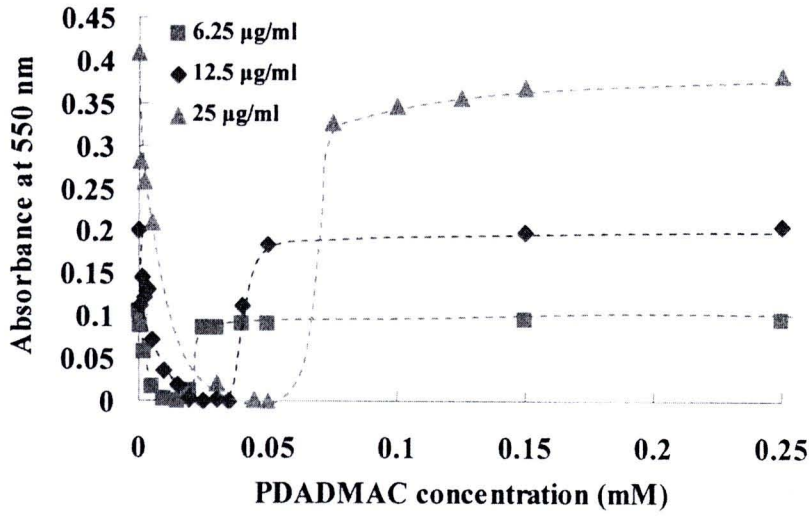

Figure 4.17 Plots of the changes in absorbance of modified MWCNT (6.25, 12.5 and 25 µg/ml) with various PDADMAC concentrations (0-0.25mM) after preparing for 1 week.

Using these plots it is possible to identify the concentration of PDADMAC that is needed to modify the surface of the MWCNT and limit its excess in solution. The amount of PDADMAC that need to be added to the MWCNT solution is proportional to the amount of MWCNT present in solution and when different carbon nanotubes concentrations (6.25, 12.5 and 25 µg/ml) were used, it can be seen on Figure 4.17 that PDADMAC concentration of 0.025 mM, 0.05 mM and 0.075 mM are respectively needed. The zeta potential of primary coating MWCNT with PDADMAC in different MWCNTs and PDADMACconcentrations was shown in Figure 4.18.

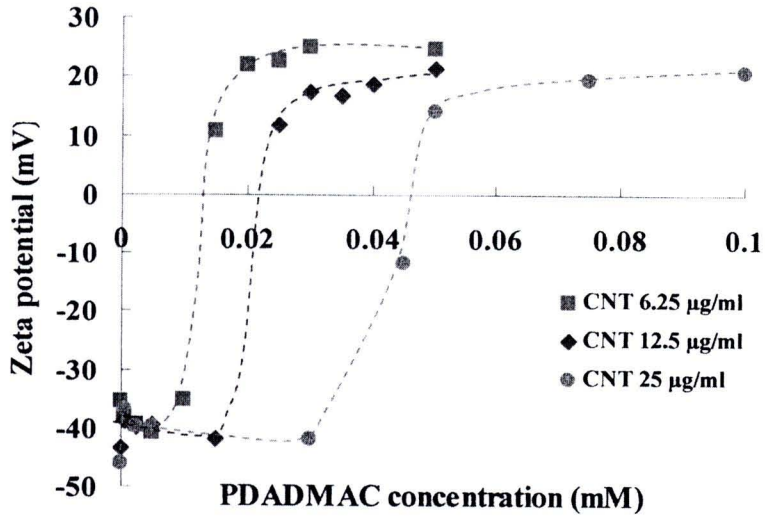

Figure 4.18 Plots of zeta potential of modified CNT 12.5, 25, 50 µg/ml with various PDADMAC concentrations.

A linear relationship between various MWCNT and PDADMAC content was found in Figure 4.19 to be equal to 0.48 mg of PDADMAC per 1 mg of CNT.

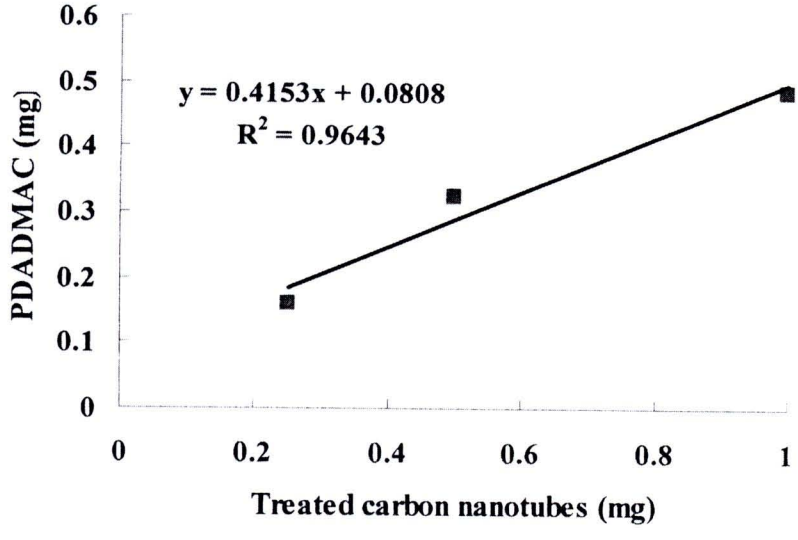

Figure 4.19 Mass ratio between PDADMAC and treated carbon nanotubes as a primary layer.

Considering the densities of the MWCNT and the PDADMAC layer to have the values of 2.1 and 1.04 g/cm^3 respectively, an average thickness of 3.5 nm per layer can be calculated. Values of 1 nm per PDADMAC monolayer after adsorption on silicon wafer have been previously reported independently of the ionic strength of the solution by Decher but these values are expected to the smaller than that on carbon nanotubes as the electrostatic interaction are much greater on silicon wafer. The layer thickness reported here is also greater probably due to the fact that some PDADMAC segments form loops in the solution leading to a higher amount of PDADMAC adsorbed. These results imply that the polyelectrolytes do not wrap perfectly around the nanotubes and form a loose coating around the nanotubes with some segment adsorbed and some extending largely in solution. This result was confirmed later using TEM imaging.

4.1.4.1.2 Stability of treated and primary coating on MWCNT in different salt concentrations and pH condition.

The stability of two modified MWCNT, treated MWCNT and MWCNT coated with PDADMAC in different salt concentration were investigated. Normally, blood in body contain NaCl ~0.15 M, for applying MWCNT as a drug carrier, it was necessary to investigate the CNT stability in various salt concentration to prove that the modified MWCNT can stabilize without any precipitation in NaCl 0.15 M. The absorbance of treated MWCNT starts decreasing at salt concentration 0.1 M and dramatically decreased when the salt concentration reach 0.15 mM (Figure 4.20, squares). While MWCNT coating with PDADMAC were stable in all range of salt concentration (Figure 4.20, diamonds). The carboxylate group of treated CNT were possibly attracted with sodium ion as a counterion to reduce the repulsion between negatively charged nanotubes and finally, aggregation by van der Waals interaction. The MWCNT coated with PDADMAC can be stable in aqeuous solution with any salt concentration because the PDADMAC was the pH independent polyelectrolyte.

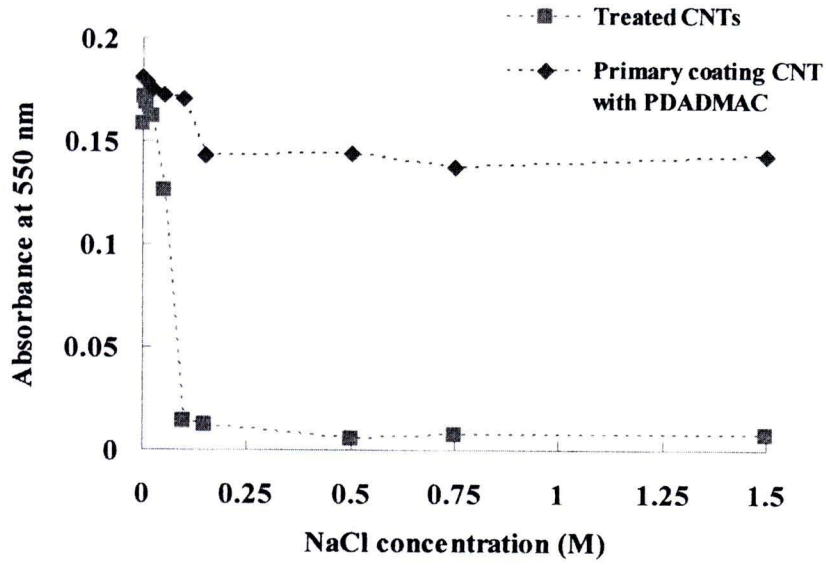

Figure 4.20 Stability of modified MWCNT, treated MWCNT and PDADMAC coated on MWCNTs, as a function of salt concentration for 1 week.

Figure 4.21 shows the stability of treated MWCNT and primary coating on MWCNT with PDADMAC after dispersed in various *pH* solutions. The carboxylic groups were different extent of deprotonation in aqeuous solution of various *pH* condition. At higher *pH*, the extent of deprotonation were increased which lead to higher carboxylate contents. *Yeong-Tarng Shieh et al.* [88] suggested that the negative charge delocalized over the two oxygen atoms in the carboxylate anion as in reaction [1] below would expel each other and this provides solubility of the treated MWCNTs in aqeuous solution.

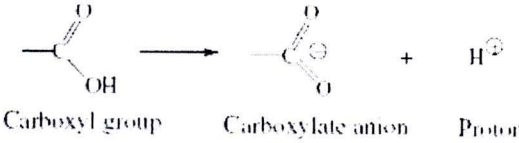

.....[1]

Although *pKa* of carboxylic acid groups equal 4.5 which means that at *pH* 4.5, the same proportion of neutral and ionized species present in solution, treated MWCNT can be stable in aqeuous solution $pH \geq 3$ while treated MWCNT were

precipitated at *pH* 2. The results agree with research work of *Barron et al.* [89]. They found that the carboxylic acid-functionalized CNTs was fully protonated in water of below *pH* 3 in which the MWCNTs were closed to neutral. The fully protonated carboxylic acid of treated CNTs were aggregated by intermolecular hydrogen bonding of carboxylic acid groups and tend to precipitate. At high *pH*, treated CNTs were stable even the *pH* of aqeuous solution equal 11. However, the ionic strength in the system were possibly increased at *pH* higher than 11 and treated CNT can be precipitated.

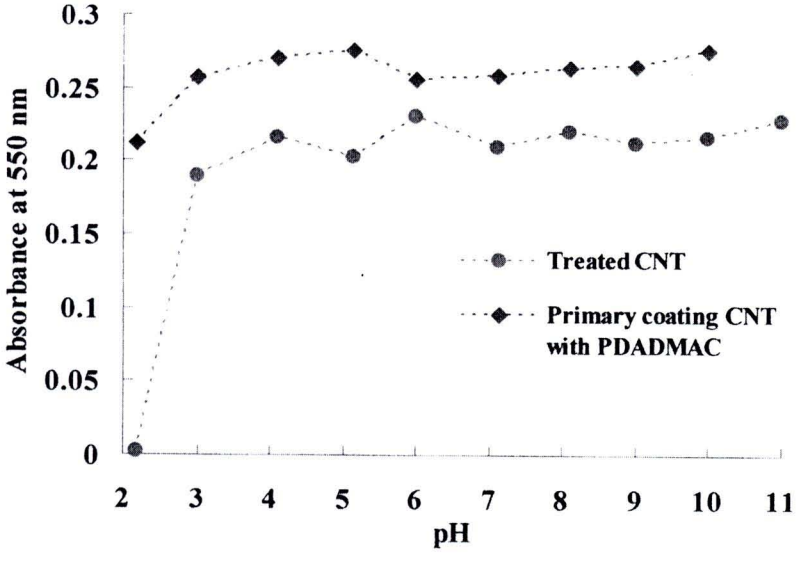

Figure 4.21 Stability of modified MWCNT, treated MWCNT and primary coating MWCNTs with PDADMAC , as a function of *pH* for 1 day.

4.1.4.2 Secondary layer coating on MWCNTs

Using the MWCNT modified with the primary layer of PDADMAC, a similar procedure was used to deposit another layer of anionic PSS. An increase in PSS concentration leads the primary coating MWCNT with PDADMAC to precipitate because the secondary coating MWCNT with PDADMAC/PSS complex with primary coating MWCNT with PDADMAC inadequate PSS concentrations. The changed of

absorbance at 550 nm in modified MWCNT solution can be observed in term of turbidity was shown in Figure 4.22. Until the PSS concentration reach to 0.04 mM, the primary coating MWCNTs can disperse in the aqeuous solution and provide the reversal of the MWCNT surface charge to negative as shown from the zeta potential's evidence in Figure 4.23. The zeta potential result confirmed that the secondary coating on MWCNT were successfully prepared.

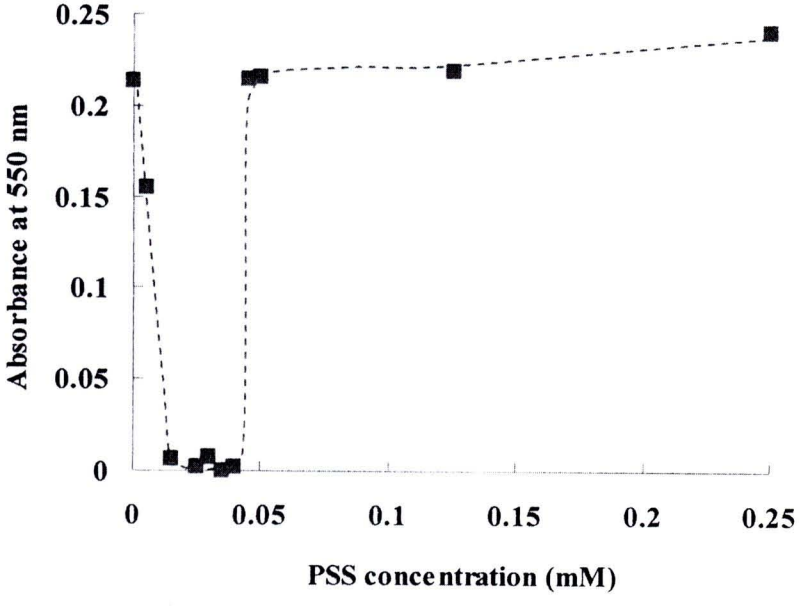

Figure 4.22 Plots of changes in absorbance of primary coating MWCNT with PDADMAC as a function of PSS concentrations, final amount of MWCNT: 12.5 μg/ml.

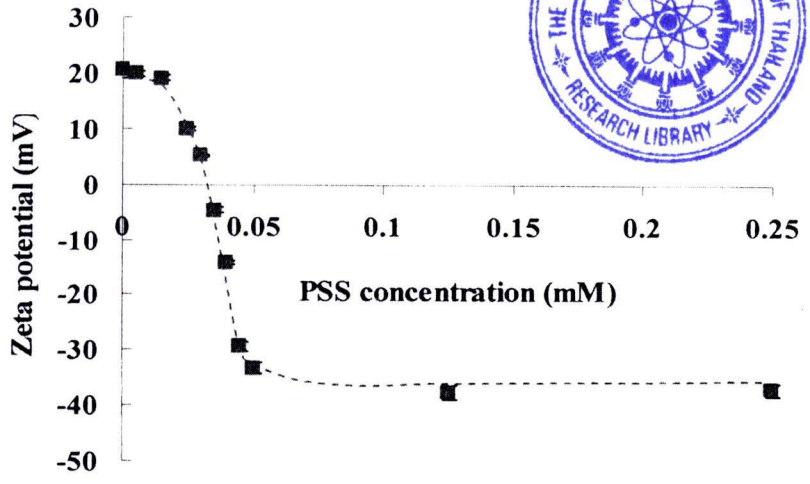

Figure 4.23 Plots of the reversal zeta potential of primary coating MWCNT with PDADMAC as a function of PSS concentrations, final amount of MWCNT: 12.5 μg/ml.

The amount of PSS added to reverse the surface charge from the PDADMAC top layer was found to be nearly equimolar than that of the previous PDADMAC layers suggesting the nearly 1:1 ratio of the polyelectrolytes for surface charge compensation. Also because the primary solution did not contain excess PDADMAC, it was possible to mix it directly with the PSS solution without the need of a centrifugation step and without the appearance of any precipitate in the solution.

4.1.4.3 Tertiary layer coating on MWCNTs

To demonstrate the usefulness of this technique a third layer of PDADMAC was deposited onto the anionic PSS coated secondary MWCNT. The benefit of this technique rely on the possible successive deposition of polyelectrolytes layers onto the MWCNT without having to centrifuge the MWCNT.

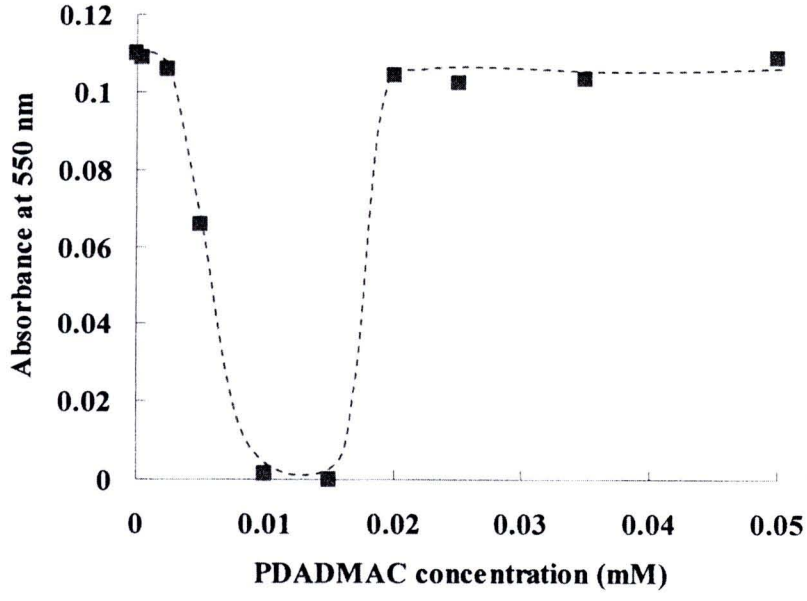

Figure 4.24 Plots of changes in absorbance of secondary coating MWCNT with PDADMAC/PSS as a function of PDADMAC concentrations, final amount of MWCNT: 6.25 μg/ml.

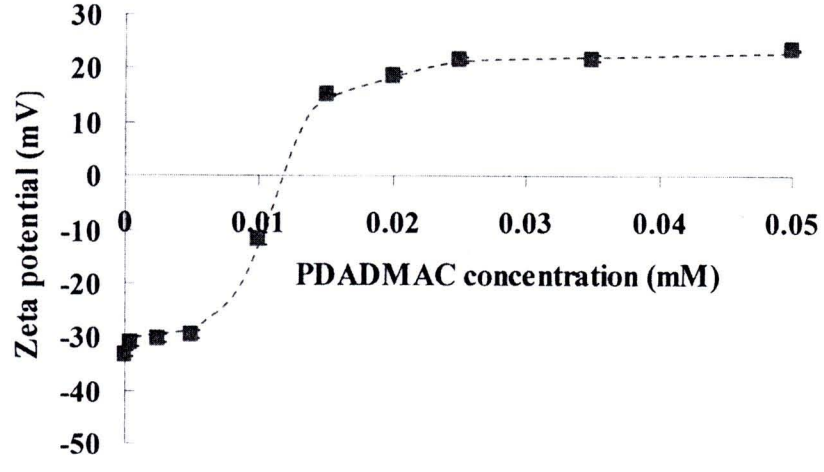

Figure 4.25 Plots of the changed in zeta potential of secondary coating MWCNT with PDADMAC/PSS as a function of PDADMAC concentrations, final amount of MWCNT: 6.25 μg/ml.

In Figure 4.24, the changes in zeta potential values are plotted for the deposition of the primary, secondary and tertiary layer as a function of the added polyelectrolyte concentrations. The zeta potential values for each layer are presented in Figure 4.25 and can be seen to alternate between positive and negative after the deposition of each layers in Figure 4.26.

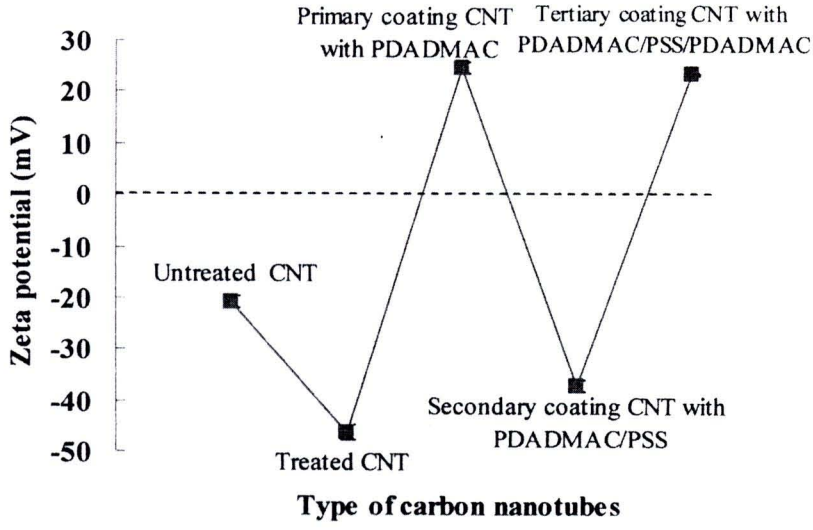

Figure 4.26 Zeta potential of untreated MWCNT, treated MWCNT, primary coating MWCNT with PDADMAC, secondary coating MWCNT with PDADMAC/PSS, and tertiary coating MWCNT with PDADMAC/PSS/PDADMAC.

Transmission electron microscopy (TEM) was used to measure the thickness of the three layers coating on the MWCNT (Figure 4.27). The calculated thickness for each deposited polyelectrolytes layers was 3.5 nm per layer which would lead to 10.5 nm of three layers coating. Evidence of the fast growth of the PEM onto the MWCNT surface can be seen from TEM images of the bare MWCNT and the 3 layers (PDADMAC/PSS/PDADMAC) coating. The multiwall carbon nanotubes used in this study have a diameter of 14 nm and the thickness of the final coating can be estimated to be 13.4 nm (+/- 2 nm) which value is closed to the calculated value from polyelectrolytes adsorption. The coating of three PDADMAC/PSS layers is thicker than the deposition on

flat silicon wafer. This is probably due to the formation of a large number of loops and tails in solution. Nevertheless this is beneficial to the coating efficiency, suggesting that the coating thickness is sufficient for drug loading and can be achieved much faster than expected from flat substrates. The layer-by-layer technique is a method of choice for the modification of MWCNT as it provides a good control over the surface chemistry and the surface charge can be tuned by the number of deposited layers. The fast growth of the PEM coating by formation of a loose structure can then be used for the selective adsorption of either cationic or anionic drugs depending on the charge of the top layer.

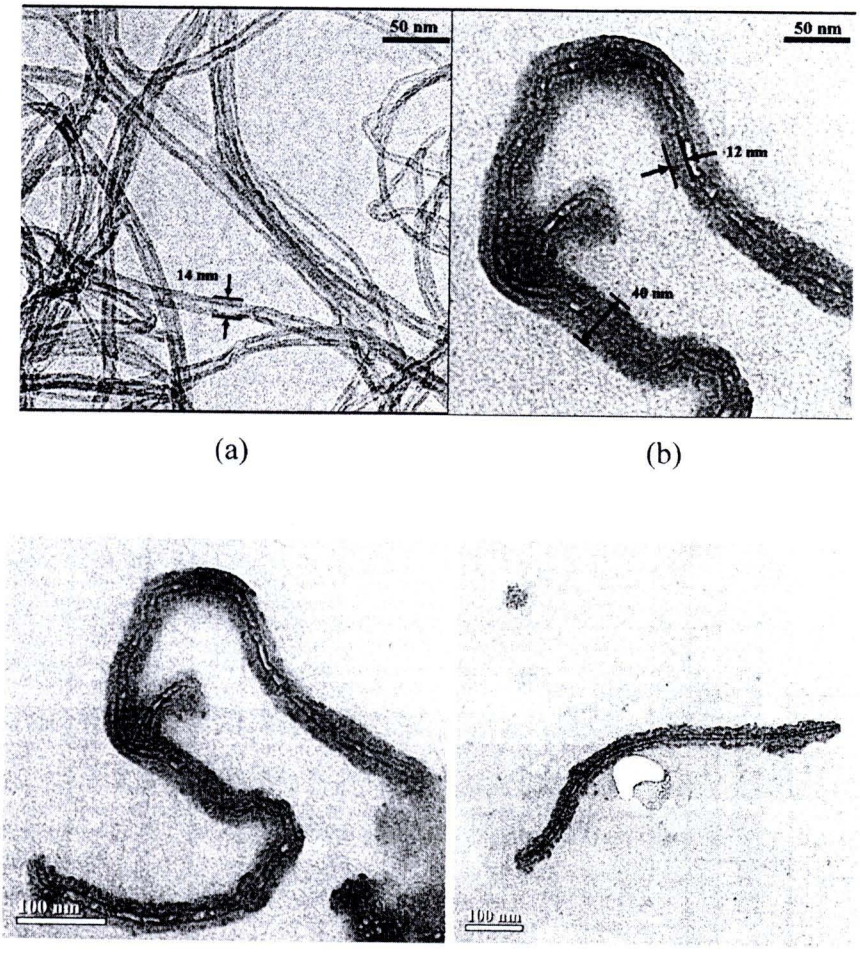

(a) (b)

(c) (d)

Figure 4.27 Transmission electron micrograph of (a) pristine MWCNT scale bar 50 nm, (b) tertiary coating MWCNT with PDADMAC/PSS/PDADMAC scale bar 50 nm, (c),(d) tertiary coating MWCNT with PDADMAC/PSS/PDADMAC scale bar 100 nm.

In conclusion, by carefully controlling the concentration of polyelectrolytes in solution, the layer-by-layer deposition of polyelectrolytes multilayers on MWCNT is simplified and do not require tedious centrifugation-sonication steps. Since the sufficient amount of PDADMAC and PSS were deposited on treated carbon nanotubes surface as a primary, secondary and tertiary layer, the modified MWCNT can then be prepared in large scale. The adsorption of the polyelectrolytes for each layers was monitored by turbidity measurement with a UV-Vis spectrophotometer and zeta potential. Using TEM imaging, the thickness of the three layers coating on the MWCNT was measured to be 13.4 nm which suggest the formation of loose polyelectrolyte network onto the MWCNT surface. This simple method can be used to coat large scales of CNT solutions for drug delivery applications.

4.2 Loading and recovery of hydrophilic model drugs of modified multiwall carbon nanotubes

4.2.1 Loading and recovery of gentian violet of treated multiwall carbon nanotubes, primary and secondary coating multiwall carbon nanotubes

Treated MWCNTs which were negative charge in 0.1xPBS buffer were coated with cationic polyelectrolyte: PDADMAC by electrostatic interaction. The insufficient concentration of PDADMAC to coat treated MWCNT lead to the aggregation between two species which were negatively charged species; uncoated MWCNT and positively charged species; PDADMAC coated MWCNT. Therefore, some treated MWCNTs were still suspended but some MWCNTs were precipitated by attracting with a slight concentration of PDADMAC. Until the aggregation between negatively charged of MWCNTs and positively charged of MWCNTs lead all of MWCNT completely precipitate in the solution, the solution become clear and lead the absorbace become nearly zero. When the concentration of PDADMAC was adequate to coat MWCNT, the modified MWCNT in solution can suspend in the solution and providing their stability in the aqueous solution. The lowest concentration of PDADMAC which provide modified MWCNT suspend in the solution was selected to prepare positively charged MWCNT as

a precursor to deposit the secondary layer as PSS in the next step. The amount of PSS added to reverse the charge from the PDADMAC top layer was found. Also because the primary solution did not contain excess PDADMAC, it was possible to mix it directly with the PSS solution without the need of a centrifugation step and without the appearance of any precipitate in the solution. To demonstrate the usefulness of this technique a third layer of PDADMAC was deposited onto the anionic PSS coated secondary MWCNT. The benefit of this technique rely on the possible successive deposition of polyelectrolytes layers onto the MWCNT without having to centrifuge the MWCNT. In Figure 4.28, the zeta potential values for each layer are compiled in and can be seen to alternate between positive and negative after the deposition of each layers in 0.1xPBS.

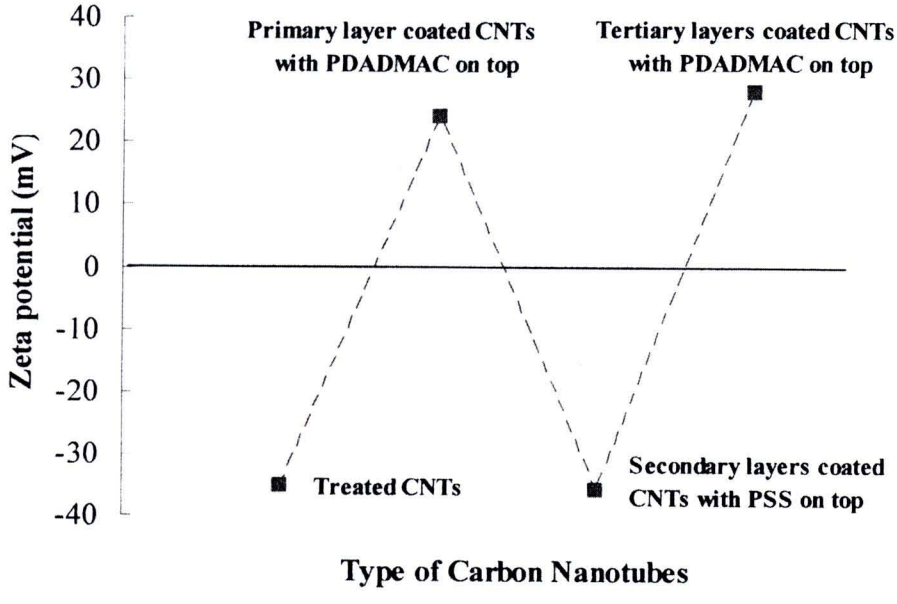

Figure 4.28 The reversal charge when the CNTs were modified with primary, secondary, and tertiary layer in 0.1xPBS buffer.

As mention above, the multilayers on the carbon nanotubes using layer-by-layer deposition technique was prepared by controlling the added polyelectrolyte

concentrations. Therefore, we can control the negative or positive charge in each layers on carbon nanotubes surface in order to load the hydrophilic drug on their surface.

Gentian violet with different concentrations was used as a cationic model drug for loading on modified MWCNT. After 24 hr of loading time, the remaining gentian violet after loading on modified MWCNT can be investigated using UV-Vis spectroscopy measurement at wavelength 585 nm. The adsorption of gentian violet on MWCNT can be observed by calculate from calibration curve of different gentian violet concentration in Figure 4.29.

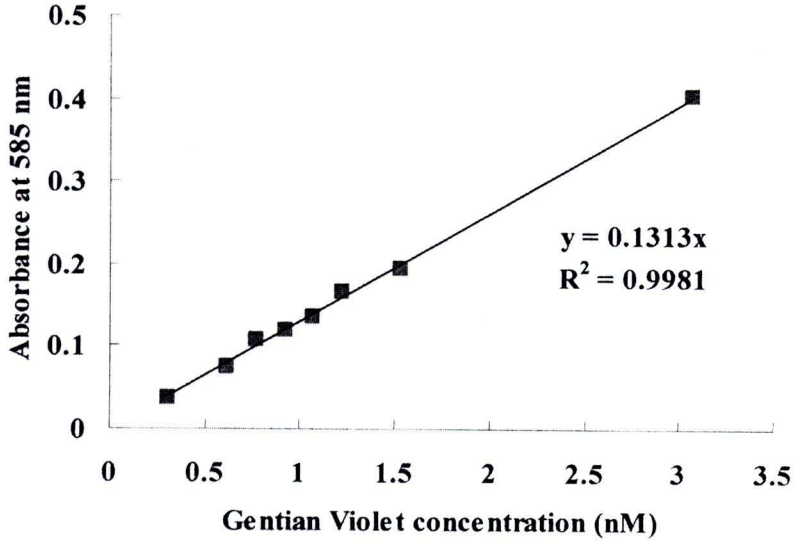

Figure 4.29 Calibration curve of gentian violet in 0.1 PBS buffer with different concentrations.

Based on our hypothesis, the cationic drug as gentian violet should be favored loading on the negative charged surface by electrostatic attraction. As we expected, negative charged surface which consist of treated MWCNT and the secondary coating MWCNT with PDADMAC/PSS can adsorb gentian violet (shown in Figure 4.30, Figure 4.32) while the primary coating MWCNT with PDADMAC can slightly adsorb in Figure 4.31.

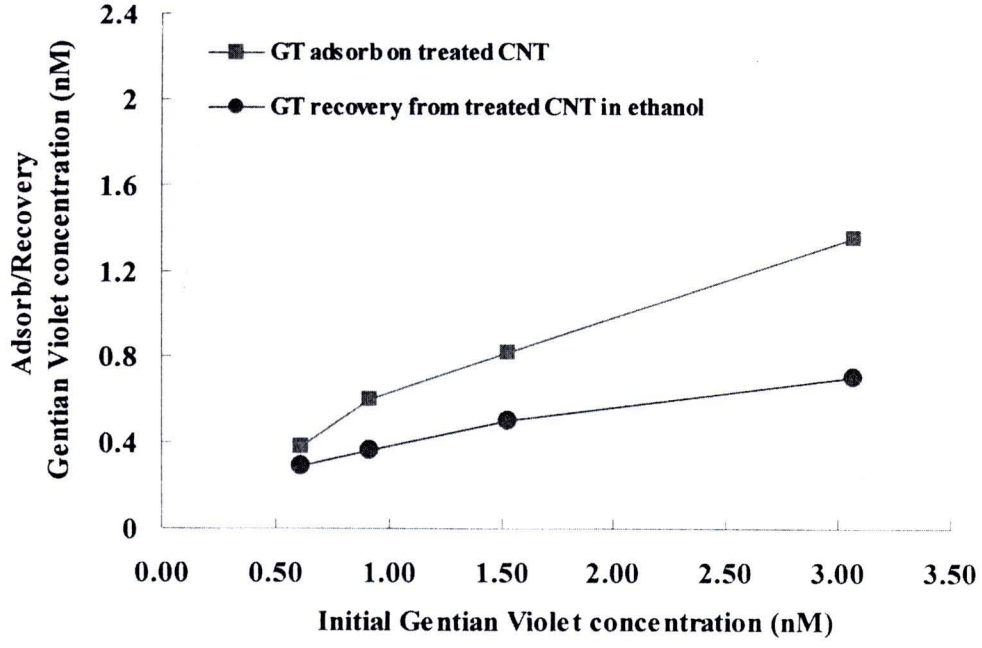

Figure 4.30 Comparison concentrations of gentian violet adsorption in 0.1 PBS and recover in ethanol from treated MWCNT.

The treated MWCNT were dispersed in the 0.1 PBS pH 7.4, gentian violet was adsorbed on treated MWCNT surface by electrostatic attraction between carboxylate groups and ammonium groups. In addition, gentian violet is possible to attach on treated MWCNT surface by pi-pi stacking between the aromatic ring of both gentian violet and the carbon nanotubes structures. As shown in the Figure 4.30, the increasing of gentian violet concentration increase in gentian violet adsorption on treated carbon nanotubes. The % loading of gentian violet can be calculated when compared with the initial gentian violet concentrations consist of 63.1, 65.9, 53.4 and 44.1%, respectively. After centrifugation process, the gentian violet adsorbed on treated MWCNT were released with ethanol by vortex, we found that the % release for recovering gentian violet from treated MWCNT was follow 76.6, 60.3, 61.3, and 52.2%, respectively. It is possible that the high concentration of gentian violet slightly favored to adsorb on the treated MWCNT surface.

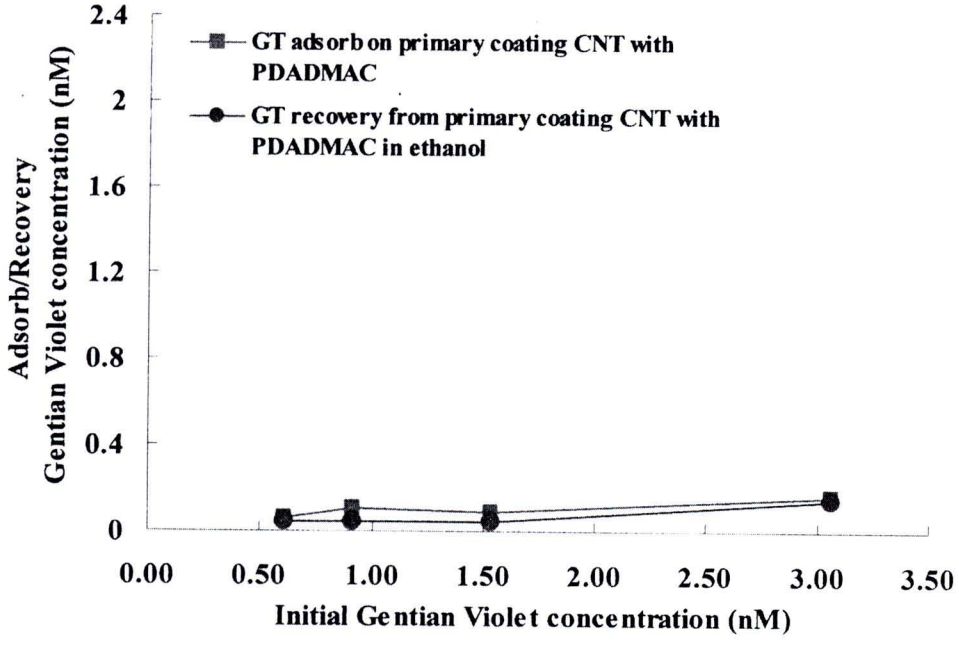

Figure 4.31 Comparison concentrations of gentian violet adsorption in 0.1 PBS and recover in ethanol from primary coating MWCNT with PDADMAC.

For the primary coating on MWCNT with PDADMAC, the result clearly showed that gentian violet are hardly adsorbed on positive MWCNT because of the repulsion of the ammonium groups between gentian violet and PDADMAC on MWCNT surface (Figure 4.31). The % adsorption were just only 10%. However, just only 10% adsorption are possibly expected that the uncompletely coated MWCNT with PDADMAC remained the small area of uncoated MWCNT which favor to adsorb gentian violet.

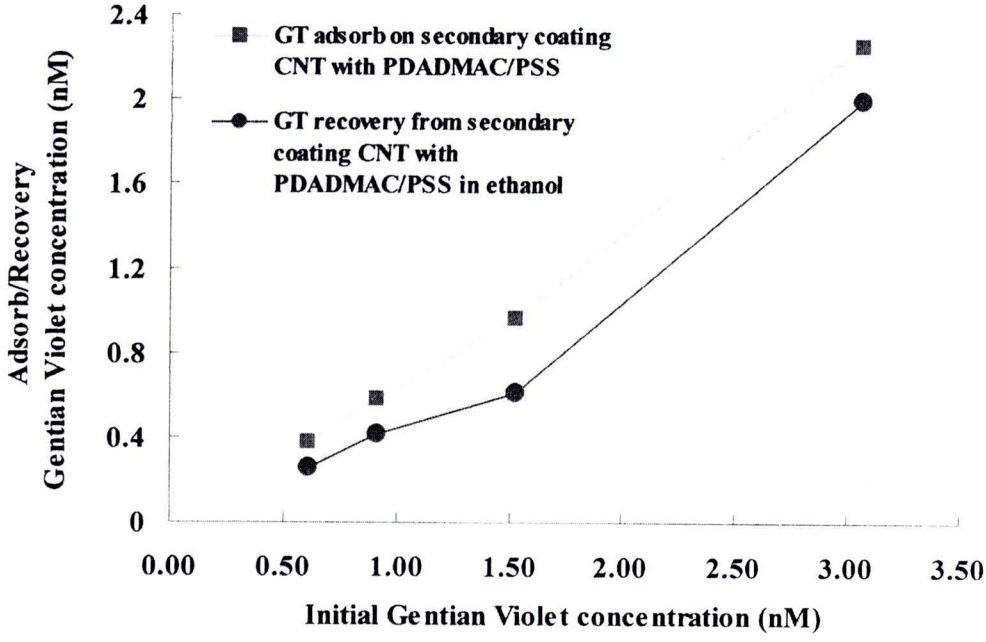

Figure 4.32 Comparison concentrations of gentian violet adsorption in 0.1xPBS and recover in ethanol from secondary coating MWCNT with PDADMAC/PSS.

According to the quaternary ammonium groups in gentian violet structure, the adsorption of gentian violet onto negative charge on surface of modified MWCNT was based on electrostatic attraction between the oppositely charged molecules. The high gentian adsorption was shown (Figure 4.32) in case of secondary coated layer which was PSS on top because the film coated on MWCNT can provide more adsorption rather than treated CNT which are having the carboxylate groups on their surface.

After loading gentian violet on modified MWCNT, the adsorption of gentian violet on modified MWCNT were quantified by releasing in ethanol which was good solvent for gentian violet. We can see that the gentian violet can be released from the modified carbon nanotubes in different concentrations. For the recovering of gentian violet from different modified MWCNT in ethanol, we found that coating MWCNT with PDADMAC and PSS on top can recover gentian violet more than treated MWCNT. This evidence showed that the affinity attraction between ammonium groups from gentian violet and negatively charged species which were carboxylate and sulfonate group was different. However, gentian violet on modified MWCNT with PDADMAC can be

released less than other condition because of less loading of gentian violet on their surface.

4.2.2 Loading and recovery of diclofenac of treated multiwall carbon nanotubes, primary and secondary coating multiwall carbon nanotubes

As mentioned treated carbon nanotubes, primary coating MWCNT with PDADMAC and secondary coating MWCNT with PDADMAC / PSS were prepared in 0.1 x PBS buffer, *pH* 7.4. Diclofenac sodium was prepared different concentrations (0.00025-0.01%) in 0.1 x PBS buffer. 20 ml of modified MWCNT were mixed with 20 ml of diclofenac in different concentrations. The solution were kept for 24 hr, after that the mixture solution were centrifuged at 14000 rpm for 15 min. The supernatant solution were measured by UV-Vis spectroscopy to determine unbound diclofenac. In this case, the modified MWCNT with any coating had no effect to load diclofenac as shown in Figure 4.33.

Diclofenac concentrations in the supernatant after centrifugation remain unchanged. This is because at *pH* 7.4, diclofenac were completely ionized and act as a salt which prefer to dissolve rather than adsorb on carbon nanotubes. Especially the negatively charged of treated MWCNT and secondary coating MWCNT possibly repel diclofenac because of their same negative charges. However, even positive charge on top surface as PDADMAC coated on MWCNT can not load diclofenac as well because the remaining diclofenac might possibly come out during the centrifugation process.

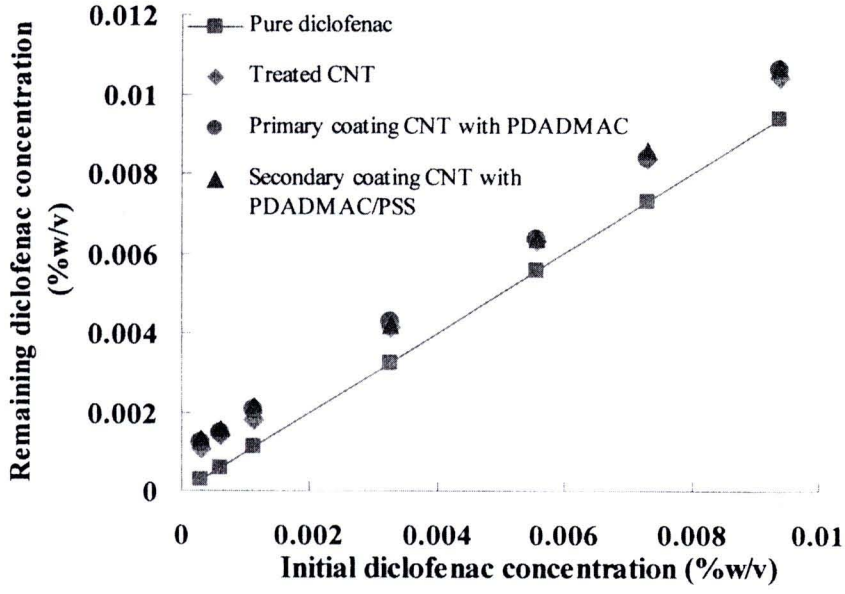

Figure 4.33 The remaining of diclofenac concentrations in 0.1 PBS after loading to modified carbon nanotubes.

Coating on carbon nanotubes with PDADMAC and PSS in term of primary and secondary layers using Layer-by-Layer technique was successful in this work. The type of charges on nanotubes is affected on drug loading efficiency. Gentian violet can be loaded on secondary coated on nanotubes surface reach to 73% whereas diclofenac sodium can not be loaded in any modified MWCNT because it's ionized and become water soluble at PBS buffer *pH* 7.4.

4.3 Cytotoxicity of modified carbon nanotubes

According to the hot issue "Toxicity of CNTs", before integrating CNTs into biomedical application, the effect of CNTs on cell have to be considered. Many publications have been proposed that CNTs are toxic while some publications still approved that CNTs are nontoxic. A wide variety of CNT toxicity results was possibly influenced from 5 main factors including size, shape, source, surface chemistry and surface area of CNTs. Therefore, toxicity issue of CNTs are still argued and discussed in wide academic research while the attempt to apply CNTs in biomedical application is

also increased. However, it is hard to find the suitable assay for cytotoxicity test, which is based on colorimetric indicator because pristine CNT surface having high hydrophobic property that possibly adsorb the dye during testing and affecting to the obtainable result. Therefore, the toxic results that we get might be false positive data.

MTT assay has been widely used as a common assay for testing cytotoxicity even there are still ongoing discussion for suitable approach. In this study, the formazan adsorption interference of untreated MWCNT and treated MWCNT was compared.

4.3.1 Interference of adsorption formazan by carbon nanotubes

The untreated MWCNT can adsorb the formazan solution more than treated MWCNT as shown in Figure 4.34. Due to the surface chemistry of pristine MWCNT which are hydrophobic, it is easily adsorbed with hydrophobic formazan more than hydrophilic surface of treated MWCNT. The result clear that pristine MWCNT can interfere with toxicity results while the treated MWCNT is less interfered although the concentrations increased.

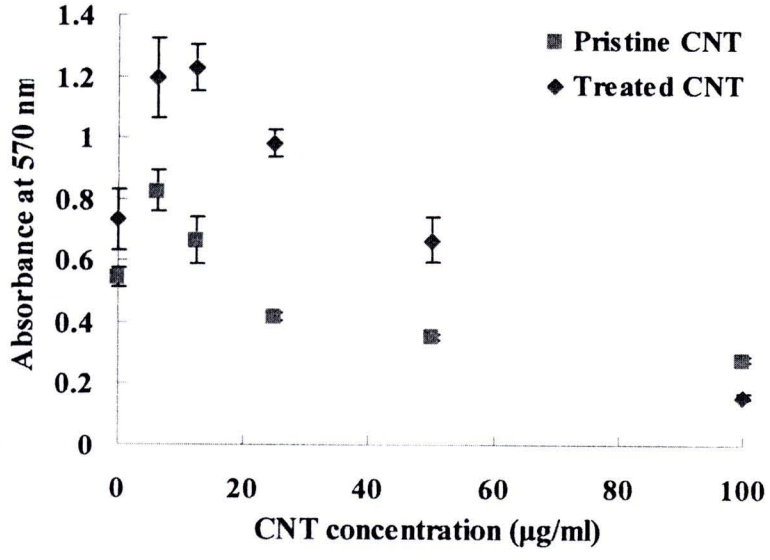

Figure 4.34 The absorbance of formazan solution at 570 nm after exposed with Untreated and treated MWCNT with various concentrations.

This result, we indicated that the treated MWCNT adsorbed formazan less than untreated MWCNT because of their charged surface. Although MWCNT still effected to the cytotoxicity results, the modified MWCNT which are water soluble, might not affect much for MTT assay and we can get more accurate results.

However, we attempt to avoid the interference of adsorption formazan from MWCNT by removing the MWCNT samples after expose with L929 cells by PBS before adding MTT solution

4.3.2 Cytotoxicity of untreated, treated, primary coating MWCNT with PDADMAC, secondary coating MWCNT with PDADMAC/PSS, tertiary coating MWCNT with PDADMAC/PSS/PDADMAC on L929 fibroblast cells

4.3.2.1 Cytotoxicity of untreated and treated MWCNT

The cytotoxicity of MWCNT was evaluated with MTT assay. After exposing pristine and treated MWCNT into L929 cells for 24 hr, the samples were washed out by PBS and MTT was exposed to the cells. The living cells can reduce MTT to Formazan crystal inside the cells while the function of death cell were lost, therefore they cannot convert MTT to formazan.

After dissolving formazan crystal with DMSO, the absorbance of formazan solutions were measured and compared with the cell control. The results (Figure 4.35) showed that the increasing of both untreated and treated MWCNT concentration from 3.125 until 12.5 μg/ml provide the nearly formazan absorbance value. When the concentration of both types of MWCNT reach 25 μg/ml, the treated MWCNT become toxic to the L929 cells while the untreated MWCNT are nontoxic.

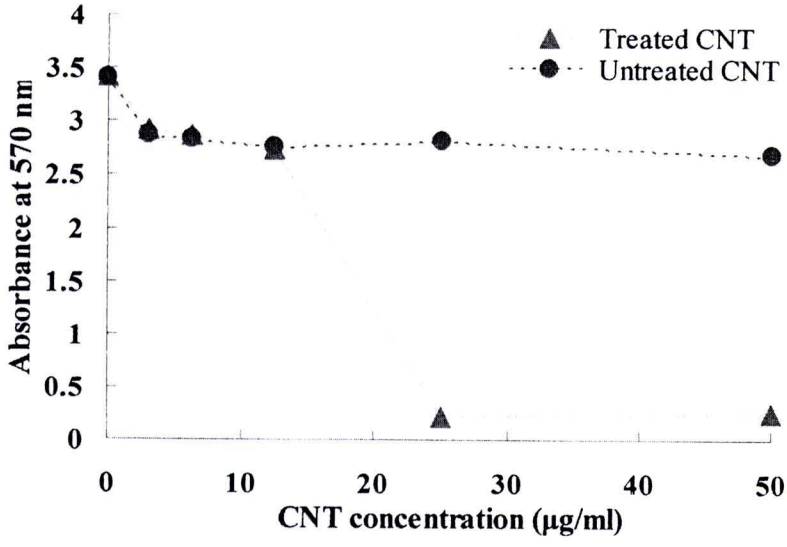

Figure 4.35 The absorbance of formazan after convert from MTT by exposing L929 cells with different concentrations of untreated and treated CNT for 24 hr.

When we calculated the % cell viability which compare with cell control as shown in Figure 4.35, the result showed that % cell viability after exposed the pristine MWCNT with different concentration provide high cell viability in range 78-83% while %cell viability of treated MWCNT provide 85-80% in treated MWCNT concentration range 3.125-12.5 µg/ml. At high concentration of treated MWCNT, the treated MWCNT reach to 25 µg/ml and 50 µg/ml, the % cell viability were dramatically decreased in to 21.4 % and 7.41%, respectively as shown in Figure 4.36. We expected that the treated MWCNT which were the shorter length provide the high dispersion because of their carboxylic groups. Therefore, treated MWCNT can easily penetrate into the cell membrane compared to the untreated MWCNT which were aggregated and having long length in term of several µm. The untreated MWCNT were hardly penetrated into the cells because of their large size of aggregation.

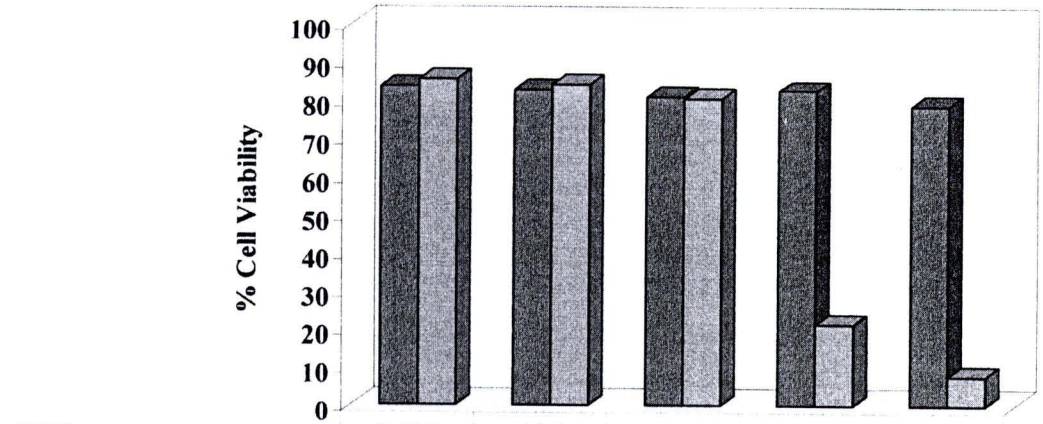

CNT concentrations (µg/ml)	3.125	6.25	12.5	25	50
Untreated CNTs	83.76	82.78	80.99	82.54	78.79
Treated CNTs	85.36	84.12	80.43	21.41	7.81

Figure 4.36 % Cell viability of L929 cell after exposed with untreated and treated MWCNT with different concentrations for 24 hr.

4.3.2.2 Cytotoxicity of primary coating MWCNT with PDADMAC, secondary coating MWCNT with PDADMAC/PSS and tertiary coating MWCNT with PDADMAC/PSS/PDADMAC

However, we attempt to modified MWCNT with different functional groups by deposition of PDADMAC and PSS in order to improve cell viability by selective functional groups. Primary (PDADMAC), secondary (PDADMAC/PSS), and tertiary (PDADMAC/PSS/PDADMAC) coating on MWCNT surface were prepared in 0.1xPBS buffer, thereafter, the modified MWCNT were separated into two type which were tested with the solultion. Another were centrifuged in order to remove the excess polymer and kept as a powder. All samples were exposed into L929 cells for 24 hr, the cytotoxicity of polyelectrolyte were tested as a control. PDADMAC and PSS with the different concentrations were exposed into L929 cells for 24 hr. An increase in PDADMAC concentration from 0.001 to 0.01 mM does not affect cell viability. However,

when the concentration of PDADMAC reach 0.05 mM, formazan absorbance dramatically decreased due to lost functions of cells (Figure 4.37).

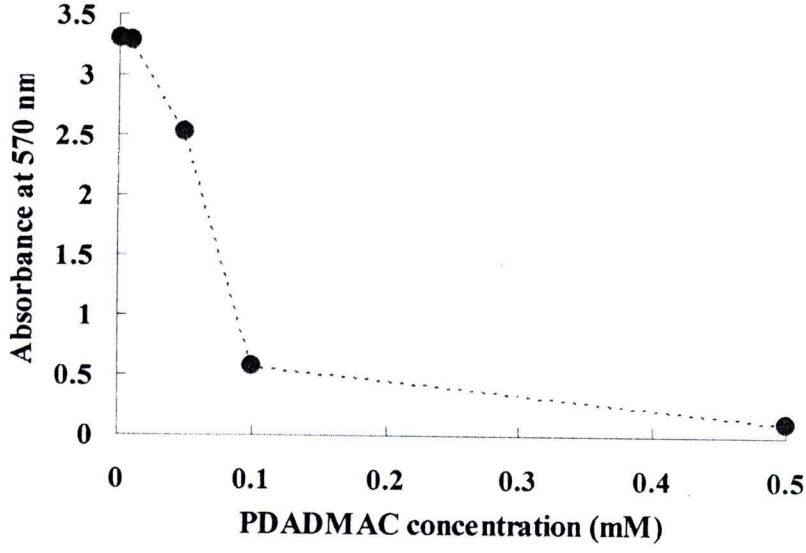

Figure 4.37 The absorbance of formazan after convert from MTT by exposing L929 cells with different concentrations of PDADMAC solultion for 24 hr.

The % cell viability can be calculated from the changed in absorbance of formazan when compare with the cell control. In Figure 4.38, % cell viability dramatically decreased after exposed PDADMAC solution reach to the concentration 0.05 mM. As shown the cell morphology after exposed PDADMAC (Figure 4.39), the L929 cells morphology were changed from the spread to shrink into round shape. Due to the synthetic polymer and their structure consist of positive charge from ammonium groups. The cationic groups can attach on the negatively charged surface of cell membrane by electrostatic attraction. In addition, the molecular weight of PDADMAC might affect the cell. However, the low concentration of PDADMAC still provide cell viability that we can use to modify CNT surface in the next step.

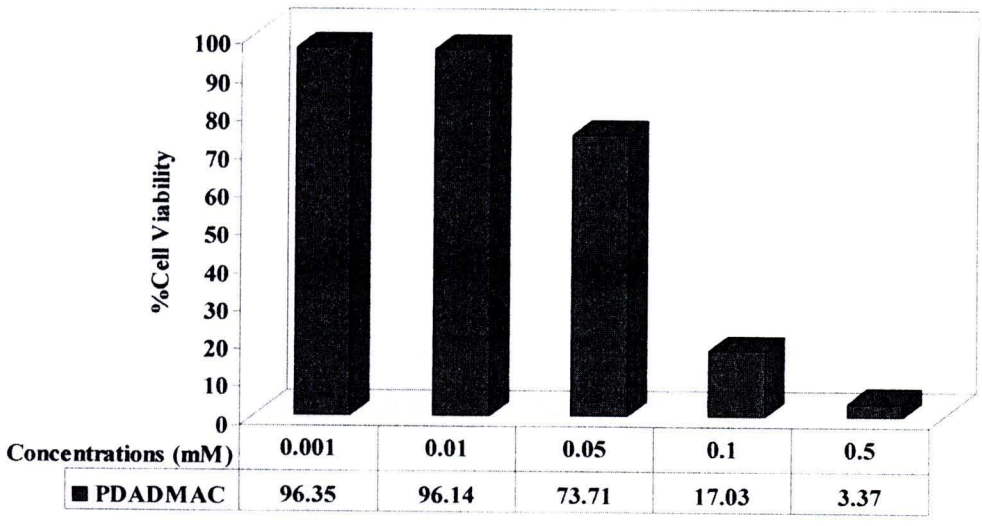

Figure 4.38 % Cell viability of L929 after exposed with PDADMAC solution with different concentrations for 24 hr.

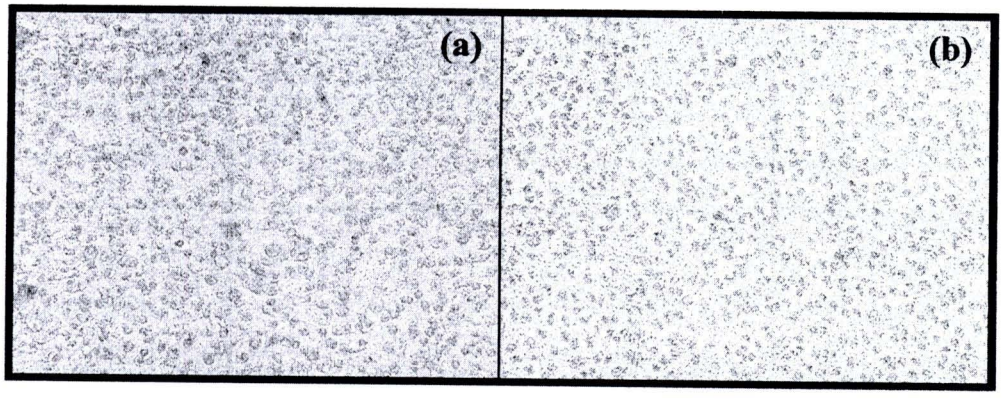

Figure 4.39 L929 cells morphology after exposed with PDADMAC concentration (a) 0.1 mM and (b) 0.5 mM for 24 hr.

PSS solution were added into L929 cells with different concentration, the cell L929 were shrink . At high concentration of PSS 0.1 and 0.5 mM were toxic to L929 cells. The cell morphology after exposed with the PSS solution were shown in Figure 4.40.

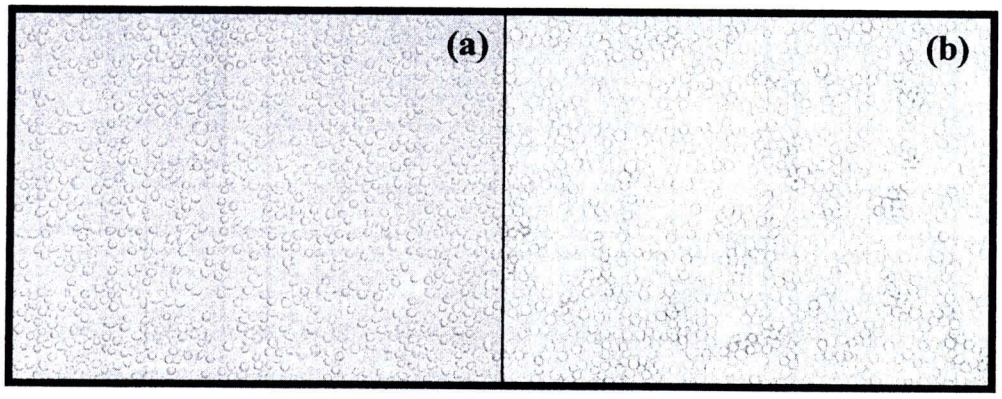

Figure 4.40 L929 cells morphology after exposed with PSS concentration (a) 0.1 mM and (b) 0.5 mM for 24 hr.

4.3.2.2.1 Cytotoxicity of primary coating MWCNT with PDADMAC, secondary coating MWCNT with PDADMAC/PSS and tertiary coating MWCNT with PDADMAC/PSS/PDADMAC : In case of solution.

The surface modification of MWCNT with polyelectrolyte as PDADMAC and PSS were used to evaluate their cytotoxicity with L929 cells by MTT assay. Three kind of coating on MWCNT which consist of primary coating MWCNT with PDADMAC, secondary coating MWCNT with PDADMAC/PSS and tertiary coating MWCNT with PDADMAC/PSS/PDADMAC were prepared in the solutions. In Figure 4.41, the MWCNT coated with PDADMAC/PSS and PDADMAC/PSS/PDADMAC with different concentrations were not significantly changed in the concentration of formazan. While the MWCNT coated with PDADMAC were toxic on L929 cells when the concentration reach to 6.25 and 12.5 μg/ml. % Cell viability in Figure 4.42 can be confirmed the toxicity of MWCNT coated with PDADMAC on top were toxic on L929 cells. This evidence might be from the effect of cationic polyelectrolyte which can attract with the negative charged of phospholipid in the cell membrane and provide the complex. In addition, the excess of polyelectrolyte in the MWCNT solution remained which might affect on cytotoxicity because PDADMAC and PSS at higher concentrations than 0.1 mM provide cytotoxicity on the cells.

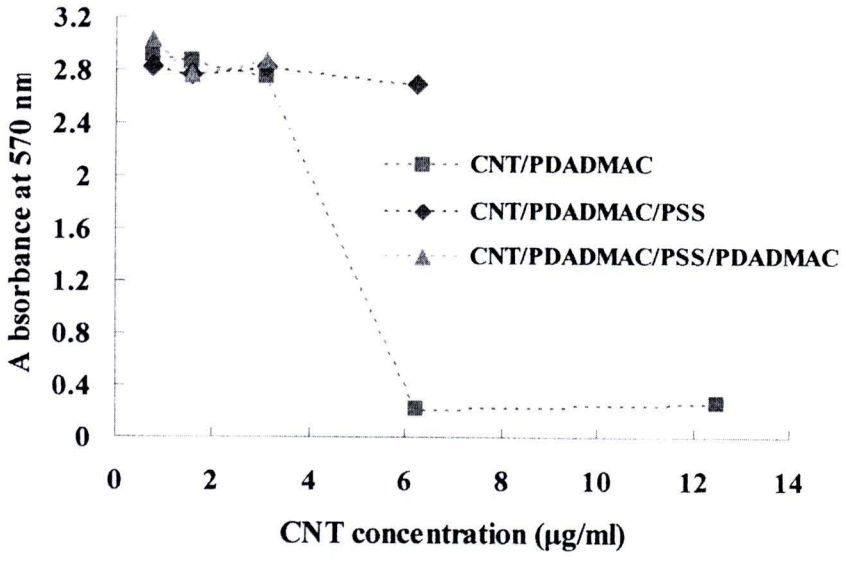

Figure 4.41 The absorbance of formazan after L929 cells were exposed with different concentrations of primary coating MWCNT with PDADMAC, secondary coating MWCNT with PDADMAC/PSS, tertiary coating MWCNT with PDADMAC/PSS/PDADMAC (In case of solution) for 24 hr.

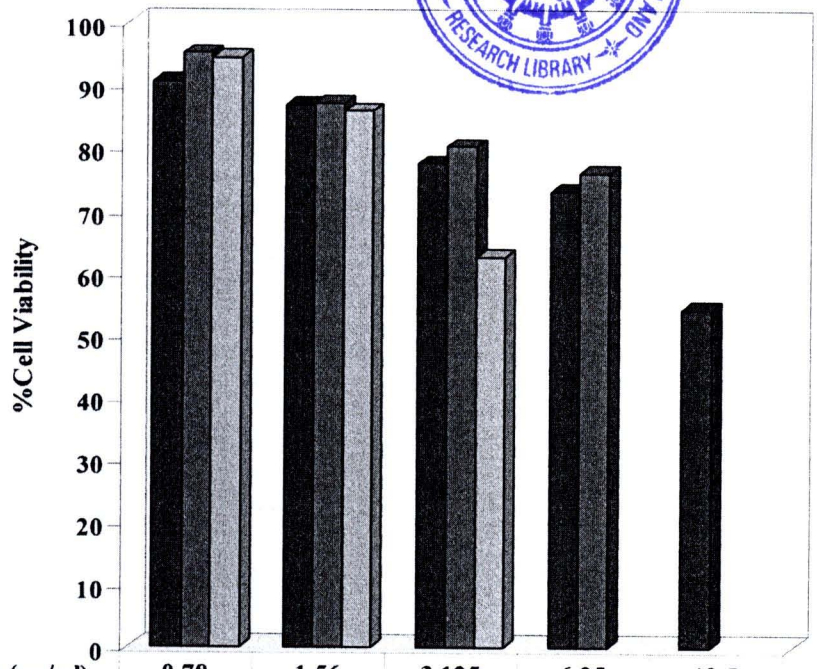

CNT concentrations (µg/ml)	0.78	1.56	3.125	6.25	12.5
Primary coating CNT with PDADMAC (solution)	90.65	86.81	77.58	73.11	54.15
Secondary coating CNT with PDADMAC/PSS (solution)	95.09	87.12	80.25	76.03	
Tertiary coating CNT with PDADMAC/PSS/PDADMAC (solution)	94.35	85.94	62.55		

Figure 4.42 % Cell viability of L929 cells after exposed with primary coating MWCNT with PDADMAC, secondary coating MWCNT with PDADMAC/PSS, tertiary coating MWCNT with PDADMAC/PSS/PDADMAC (In case of solution) with different concentrations for 24 hr.

Cell morphology of L929 after exposed with modified MWCNT with different functional groups and different concentrations was shown in the Figure 4.43

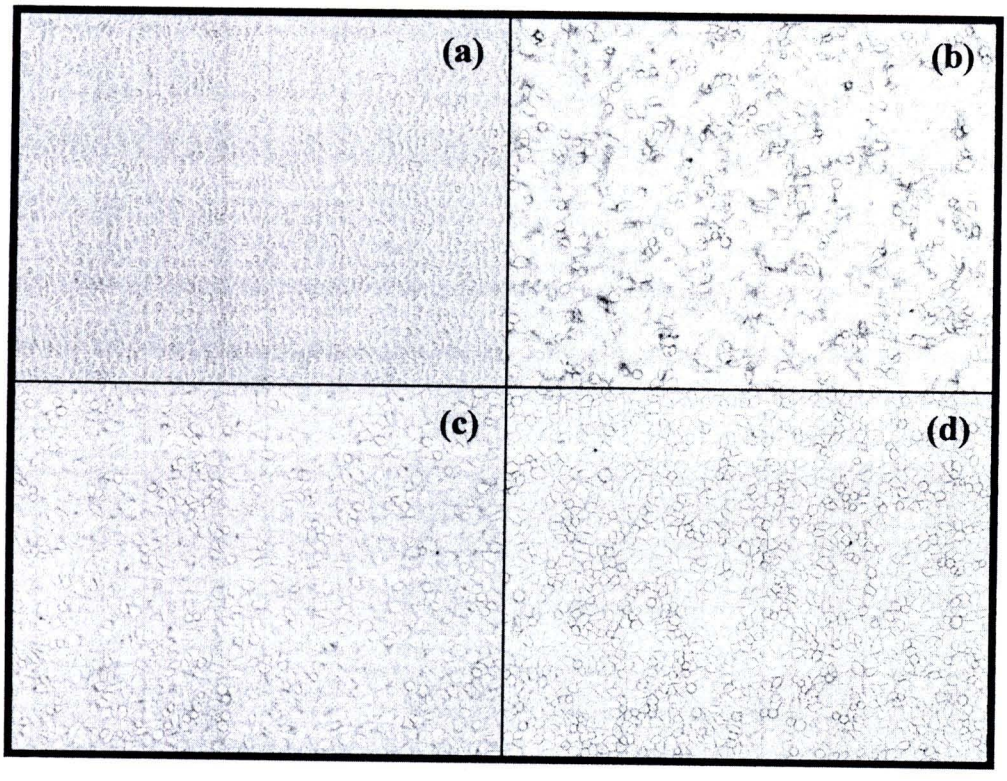

Figure 4.43 L929 cells morphology, (a) Cell control (b) Cell after exposed with primary coating MWCNT with PDADMAC 12.5 μg/ml, (c) secondary coating MWCNT with PDADMAC/PSS 6.25 μg/ml, and (d) tertiary coating MWCNT with PDADMAC/PSS/PDADMAC 3.125 μg/ml.

4.3.2.2.2 Cytotoxicity of primary coating MWCNT with PDADMAC, secondary coating MWCNT with PDADMAC/PSS and tertiary coating MWCNT with PDADMAC/PSS/PDADMAC : In case of powder.

However, the modified MWCNT with polyelectrolyte PDADMAC and PSS were centrifuged with 4000 rpm in order to remove the excess polyelectrolyte. The modified MWCNT were redispersed in DMEM which consist of the amino acid and exposed into L929 cells. The results were shown in Figure 4.44, there is no change in the absorbance of formazan with an increase in concentration of MWCNT. Figure 4.45 showed that %cell viability does not change because it is no excess polyelectrolyte which

effect on the cell toxicity. The disadvantage of the centrifugation process was that the MWCNT were densely packed and hardly redisperse in solution. Therefore, the aggregation of modified MWCNT was hardly penetrated into L929 cells. Cell morphology after exposed modified MWCNT were illustrated in Figure 4.46.

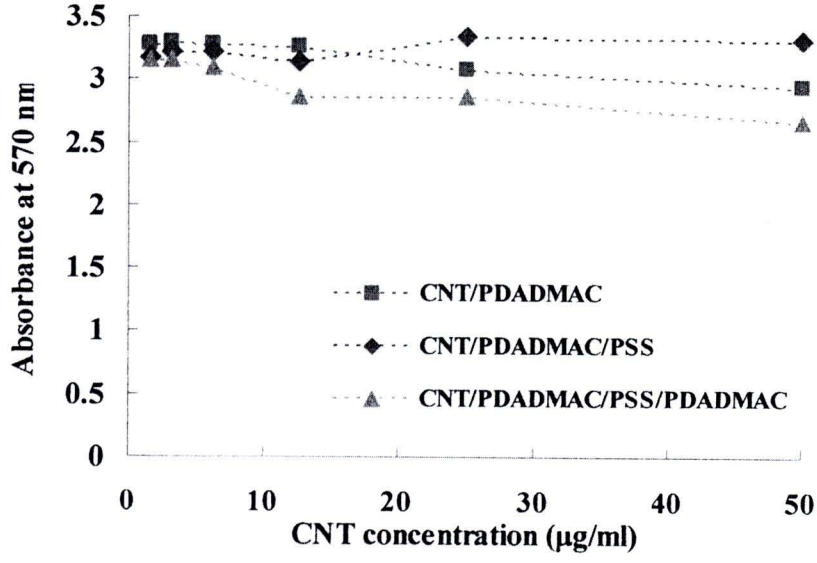

Figure 4.44 The absorbance of formazan after L929 cells were exposed with different concentrations of primary coating MWCNT with PDADMAC, secondary coating MWCNT with PDADMAC/PSS, tertiary coating MWCNT with PDADMAC/PSS/PDADMAC (In case of powder) for 24 hr.

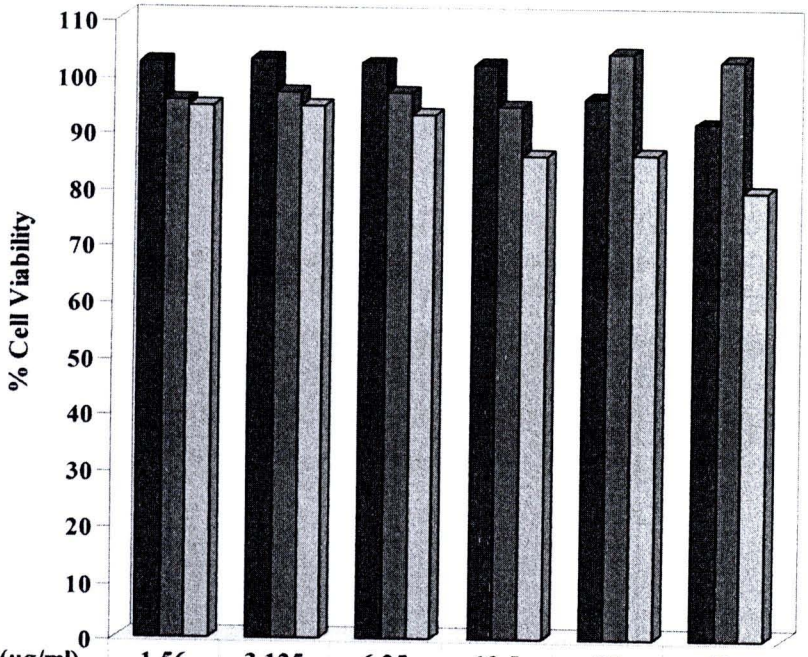

CNT concentrations (µg/ml)	1.56	3.125	6.25	12.5	25	50
Primary coating CNT with PDADMAC (powder)	102.12	102.65	101.91	101.69	95.83	91.48
Secondary coating CNT with PDADMAC/PSS (powder)	95.21	96.59	96.62	94.3	103.8	102.73
Tertiary coating CNT with PDADMAC/PSS/PDADMAC (powder)	94.38	94.39	92.91	85.59	85.97	79.5

Figure 4.45 % Cell viability of L929 cells after exposed with primary coating MWCNT with PDADMAC, secondary coating MWCNT with PDADMAC/PSS, tertiary coating MWCNT with PDADMAC/PSS/PDADMAC (In case of powder) with different concentrations for 24 hr.

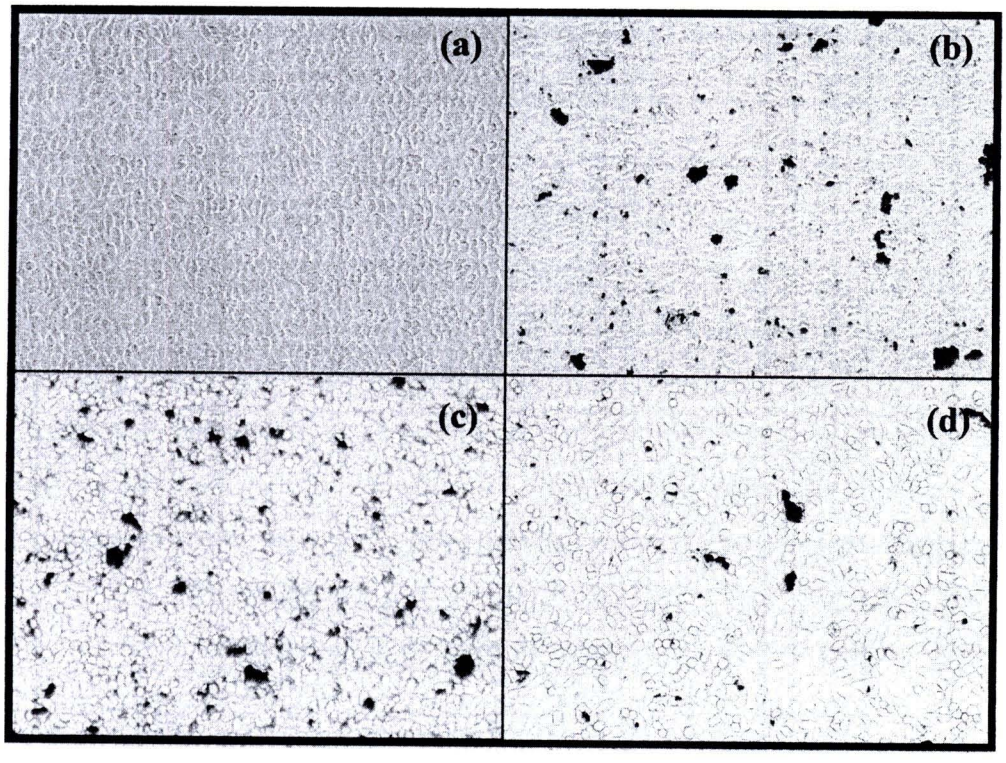

Figure 4.46 L929 cells morphology, (a) Cell control (b) Cell after exposed with primary coating MWCNT with PDADMAC 50 μg/ml, (c) secondary coating MWCNT with PDADMAC/PSS 50 μg/ml, and (d) tertiary coating MWCNT with PDADMAC/PSS/PDADMAC 50 μg/ml.